Toxicology Reports 10 (2023) 155–170

Contents lists available at ScienceDirect

Toxicology Reports

journal homepage: www.elsevier.com/locate/toxrep

Interactions of alcohol and combination antiretroviral (cART) drug in diabetic male Sprague Dawley rats: Hippocampal perturbations and toxicosis

Jaclyn Asouzu Johnson *, Robert Ndou, Ejikeme Felix Mbajiorgu

School of Anatomical Sciences, University of the Witwatersrand, Faculty of Health Sciences Johannesburg, South Africa

ARTICLE INFO

Handling Editor: Prof. L.H. Lash

Keywords:
Diabetes
Hippocampus
Neurogenesis
Antiretroviral
Alcohol
Histopathology
Toxicosis

ABSTRACT

Hippocampal pathology in diabetes is constantly investigated but the resultant health impact of the concomitant presence of alcohol and combined antiretroviral therapy (cART) in diabetes requires further studies to delineate toxicities inimical to hippocampal normal function. Forty-eight male Sprague Dawley rats were divided into eight groups (n = 6): negative control (NC), alcohol (AL), cART (AV), alcohol-cART (AA), diabetic control (DB), diabetes-alcohol (DAL), diabetes-cART (DAV), and diabetes-alcohol-cART (DAA) exposure groups. Following diabetes induction and sub-chronic (90 days) treatment exposure, hippocampal homogenates were profiled for pro-inflammatory cytokines and oxidative stress (MDA and GPx) using immunoassay, while apoptotic genes (BAX, Bcl_2, and Caspase-3), insulin receptor genes (INSR and IRS-1), and blood-brain barrier (BBB) junctional proteins (claudin-5, and occludin) gene expression were assessed using qPCR. Histomorphology of hippocampal neuronal number, nuclei area, and volume of dentate gyrus and neurogenesis were accessed using Giemsa stain, Ki67, and DCX histochemistry respectively. A central hippocampal effect that underpins all treatments is the reduction of DG neuronal number and antioxidant (GPx), highlighting the venerability of the hippocampal dentate gyrus neurons to diabetes, alcohol, cART, and their combinatorial interactions. Additionally, elevated BAX, Bcl_2, and IRS1 mRNA levels in the DAL group, and their downregulation in AA, suggests IRS-1-regulated apoptosis due to differential modulating effects of alcohol treatment in diabetes (DAL) in contrast to alcohol with cART (AA). Although the interaction in AA therapy ameliorated the independent alcohol and cART effects on MDA levels, pro-inflammatory cytokines, and DCX, the interaction in AA exacerbated a deficiency in the expression of INSR, IRS-1 (insulin sensitivity), and BBB mRNA which are implicated in the pathogenies of diabetes. Furthermore, the diabetic comorbidity groups (DAV, DAL, and DAA) all share a central effect of elevated hippocampal oxidative stress, BAX, and Caspase-3 mRNA expression with the reduced number of hippocampal neurons, dentate gyrus volume, and neurogenesis, highlighting neurodegenerative and cognitive deficiency implication of these comorbidity treatments. Considering these findings, assessment of hippocampal well-being in patients with these comorbidities/treatment combinations is invaluable and caution is advised particularly in alcohol use with cART prophylaxis in diabetes.

1. Introduction

Type 2 diabetes (T2D) is one of the most common chronic health and socio-economic problems in South Africa and globally [59,73]. Diabetes is classified into the general categories of type 1, type 2, gestational diabetes, and specific type of diabetes [6]. Specific diabetes includes monogenic diabetes syndrome, diseases of the exocrine pancreas, and recently drug or chemical-induced diabetes such as disease (for example Covid-19) associated diabetes [1]. Incidentally, combined antiretroviral therapy (cART), the first-line drug for the treatment of HIV/AIDS has been associated with metabolic syndrome and the pathogenesis of type 2 diabetes [12,45]. Additionally, lifestyle factors such as alcohol use/abuse can exert chemotoxicity, resulting in diabetes [14,25]. Consequently, chronic cART-induced diabetes is gradually becoming prevalent as a high proportion of individuals who are on chronic medications and regularly use alcohol may develop diabetes [23,36]. As reports indicate the continued spread of HIV/AIDS and cART in sub-Saharan Africa and globally [68,71], it is therefore of interest to

* Corresponding author.
E-mail addresses: jaclyn.johnson@wits.ac.za (J. Asouzu Johnson), robertndou@smu.ac.za (R. Ndou), ejikeme.mbajiorgu@wits.ac.za (E.F. Mbajiorgu).

https://doi.org/10.1016/j.toxrep.2023.01.009
Received 4 November 2022; Received in revised form 7 January 2023; Accepted 19 January 2023
Available online 20 January 2023

investigate the possible combined impact of cART and alcohol intake in diabetic individuals. Furthermore, this alcohol cART co-morbidity under a diabetic condition may require multiple drug therapy investigations to elucidate its health impact, especially on glucose-sensitive organs such as the brain.

The hippocampus is sensitive to insulin signalling and glucose homeostasis for the regulation of cognitive, memory, neurogenesis, and neuroprotective functions [34,53,70]. Hippocampal neurons and endothelial cells contain several membrane-bound insulin receptors (INSR), which recruit intracellular adapter proteins; insulin receptor substrate (IRS-1) in the canonical insulin signalling and mediate glucose uptake into cells [75]; [21]; [50]. Additionally, the penetration of drugs, chemicals, and inflammatory cytokines produced by microglial cells, into the hippocampus is tightly regulated [13,32] through junctional blood-brain barrier (BBB) proteins claudin-5 and occludin [19] located on hippocampal endothelial cells. However, the presence of chemical toxicants can disturb the BBB structural integrity. Therefore, the presence of alcohol, cART and diabetes may induce perturbations in the normal physiological regulation of insulin receptors, BBB proteins, and cytokines which may induce a cascade of events associated with oxidative stress, apoptosis, and compromised neurogenesis which are all independently reported in alcohol, cART, and diabetes [26,54,67,72]. Similarly, diabetes, alcohol, and cART are independently associated with hippocampal and cognitive impairment [44,46,58], and consequently their comorbidity (cART+ diabetes) showed an exacerbated effect [5]. However, the interaction of alcohol use with diabetes (alcohol +diabetes), the concomitant presence of cART and alcohol in the normal rat hippocampus (cART +alcohol), and in the diabetic hippocampus (alcohol + cART + diabetes) remains unclear. Therefore, the adverse effects of the co-presence of alcohol, cART, and diabetes on some molecular and histopathological parameters in the hippocampus that may negatively impact cognition require further elucidation for possible related neuropathological effects, especially as it relates to diabetic individuals living with HIV/AIDS, who consume alcohol regularly.

Clinical management of comorbidity patients often requires multiple drug therapy which commonly is associated with several independent side effects but cumulative drug-drug interaction between therapies [30, 39] could together become detrimental to overall patient health. Therefore, this study is designed to investigate the dual presence of cART administration and alcohol intake in type 2 diabetes for its attendant hippocampal effects relative to oxidative stress, neurogenesis and hippocampal insulin receptors. Additionally, we investigated the differential hippocampal toxicosis that may exists following the interaction of alcohol with cART, and the interactions of either alcohol or cART with diabetes in contrast to the hippocampal toxicity independently induced by alcohol, cART and diabetes.

Additionally, the use of an HIV naïve model in the current study excluded the possible impact (pathologies) associated with the presence of HIV on tissue-drug-disease interactions and enabled the toxicity of diabetes + alcohol + cART combinations to be studied and documented. We hypothesized that oxidative stress and neuroinflammation are central to most of the hippocampal pathologies induced. We used hippocampal tissue homogenates for the analysis of pro-inflammatory cytokines, oxidative and anti-oxidative enzymes. To evaluate the diabetogenic, metabolic, and neurodegenerative effects of these treatments specifically on the hippocampus, the molecular expression for insulin receptors and apoptosis in the hippocampus was described. We illustrate the histopathology of our molecular and biochemical findings by evaluating the impact of these treatments on the histomorphometry and immunostaining of neurons for associated toxicosis such as atrophy and deficit neurogenesis. We showed a novel effect of deficit antioxidant and dentate gyrus neurons as a uniform pathological effect across all different combinations of treatments.

2. Materials and methods

2.1. Chemicals

Oxidative stress markers were assessed using a malondialdehyde (MDA) Colorimetric assay kit: TBA method (Elabscience, Houston, Texas USA; E-BC-K025-M), and Glutathione Peroxidase (GSH-Px) Activity Assay Kit (Elabscience, Houston, Texas USA; E-BC-K096-M WST-1 Method). For PCR, TRIzol reagent (Merck; T9424), iso-propanol (Merck; B6916), cDNA using a high-capacity cDNA RT kit (Applied Biosystems; 4368814), Power Up SYBER Green Master Mix (Applied Biosystems; A25742; Austin, Texas, USA), Forward and Reverse Primer were procured from Inqaba Biotechnical industries (Hatfield, Pretoria, South Africa).

2.2. Animal housing

Forty-eight adult male Sprague Dawley rats were housed separately under clean conditions in cages. For the duration of the experiment, the rats had free access to drinking water or alcohol, and rat chow according to their allocated group treatment. Daily water or alcohol intake and weekly normal rat chow consumed in treated and untreated animals were measured by recording the amount of water or alcohol remaining using a measuring cylinder and weighing the remaining rat chow. The rats were weighed weekly, and non-fasting glucose tests, biweekly fasting glucose tests, and monthly oral glucose tolerance tests were carried out.

2.3. Experimental design

The rats were divided into eight groups (n = 6), the first four groups consist of non-diabetic animals and include; Negative control, untreated animals (NC), alcohol alone, received 10% alcohol in distilled water v/v ad libitum (AL), cART alone, received only antiretroviral medication 23.22 mg /Kg body weight daily as an extrapolated daily recommended cART dose (containing efavirenz 600 mg+ emtricitabine 200 mg+ tenofovir 245 mg) in gelatine cubes (AV), alcohol and cART, received the same dose of alcohol and cART (AA). The gelatine route of administration used in the present study was chosen to mimic the recommended oral route of administration of cART. The animals body weight was used to calculate the equivalent dose of cART which was added to gelatine pellets and daily fed to the animals orally. The other four groups consist of animals in which diabetes was induced using previously reported adapted protocol involving streptozotocin and fructose feeding [5,74]. These diabetic groups include, diabetic control, diabetic with no treatment (DB), diabetes and alcohol administration (DAL), diabetes and cART treatment (DAV), and diabetes, alcohol, and ART (DAA), all treatments commenced with the rats at 13 weeks of age-old and were carried out for 90 days after which animals were terminated, brains excised, and One hemisphere was fixed in 0.4 paraformaldehyde for histology and the other hemisphere was stored at − 80°C for immunoassay and molecular analysis.

2.4. Quantitative qPCR for junctional proteins, insulin receptors, and apoptotic markers

2.4.1. RNA extraction

From each brain sample, total RNA was extracted by homogenizing samples in TRIzol reagent (Merck; T9424) at a ratio of 30 mg tissue to 1000 μl Tri-reagent using a handheld tissue grinder G-50 (Coyote Bioscience, Jiangsu, China). The homogenates were vortexed for 15 s, followed by 200 μl of chloroform vortexed again and allowed to stand for 3 min at room temperature. The samples were centrifuged at 14,000 rpm for 15 min, the supernatant was collected, and 500 μl iso-propanol (Merck; B6916) was added and centrifuged at 14,000 rpm for 15 min. The supernatant was decanted and 1000 μl of 75% alcohol was added to

the pellet and centrifuged at 8000 rpm for 5 min. Alcohol was poured off and pellets were resuspended in RNAase-free water, heated at 60 °C, cooled then stored at − 80°C for further analysis. Subsequently, the RNA samples were analysed using a Nano-Drop® spectrophotometer, Series ND-100 to determine the RNA concentration and purity, thereafter RNA samples were stored at 80 °C.

2.4.2. cDNA synthesis

RNA samples were diluted according to their concentrations to a final concentration of 50 μg/μl. Total RNA was used in a reverse transcriptase reaction to synthesize cDNA using a high-capacity cDNA RT kit (Applied Biosystems; 4368814). Ten microlitres of 2x RT master mix and 10 μl of RNA samples were pipetted into each well of a 96-well plate, which were centrifuged at 2500 rpm for 2 min. The thermocycler for a reaction volume of 20 μl was set at 25 °C for 10 min, 37 °C for 60 min x2, 85 °C for 1 min, and 4 °C for infinity.

2.4.3. qPCR experiment

The standard guidelines and minimum information for publication of quantitative real-time PCR experiments (MIQE) were followed. The samples, their relevant controls, and inter-plate calibrators were organized in triplicates. Quant studio 1, 96 well plate detection system (Thermofisher Scientific, Massachusetts, USA) was set up to run quantitative PCR expression of BAX, Bcl_2, claudin-5, Caspase-3, INSR, IRS-1, and occludin in the cDNA samples. Each 12 μl PCR well contained 1.52 μl of RNAase- free water, 6 μl Power Up SYBER Green Master Mix (Applied Biosystems; A25742; Austin, Texas, USA), 0.24 Forward and Reverse Primer, and 4 μl diluted cDNA samples. Thermocycler conditions were set for a reaction volume of 12 μl, the hold step was set at 50 °C for 2 min, 95 °C for 2 min (X40 cycles), the PCR step was set at 95 °C for 15 s, 60 °C for 1 min, 72 °C for 1 min, and melt curve step was sat at 95 °C for 15 s, 95 °C for 15 s, 60 °C for 1 min and 95 °C for 15 s. Two housekeeping genes (β actin and GAPDH) were used to control for error and all primers were procured from Inquaba Biotechnical industries (Hatfield, Pretoria, South Africa). Samples were quantified by a standard curve and the calculation of the expression fold for each gene of interest was by the ΔΔ CT method. The primer pair sequence for each gene of interest and housekeeping gene was designed on the IDT website and verified using the Oligoanalyser tool (Table 1).

2.5. Enzyme-linked immunoassay of proinflammatory cytokines (IL-1α, IL-6, TNFα) and oxidative stress markers (GPX, and MDA)

Dissected brain samples from each hemisphere per animal were homogenized and used were used to run an enzyme-linked immunosorbent assay for proinflammatory cytokines (Rat IL-1α, Rat IL-6, Rat TNFα) according to the manufacturer's protocol (Elabscience, USA; E-EL-R0011, E-EL-R0015, E-EL-R0019 respectively). Oxidative stress markers were assessed using a malondialdehyde (MDA) Colorimetric assay kit: TBA method (Elabscience, Houston, Texas USA; E-BC-K025-M), and Glutathione Peroxidase (GSH-Px) Activity Assay Kit (Elabscience, Houston, Texas USA; E-BC-K096-M WST-1 Method). All samples were diluted 1:2, all standards, and run-in duplicates. The optical density (OD) values were read at 450 nm. The analysis for MDA was according to the TBA colorimetric method following the manufacturer's protocol, the concentration was calculated in μmol/g protein. The OD was read at 620 nm using an Anthos 2010, 96 well plate reader coupled to an ADAP software. OriginPro software was used to calculate the concentration of cytokines in the samples from obtained OD values according to the manufacturer's directions in pg/ml. The total protein concentration for each sample of brain homogenate was tested using Bradford reagent., The standards were made up in bovine serum albumin (BSA), and the calculated concentration of protein in each sample was applied in calculating the final concentration of cytokines (pg/mg of protein).

Table 1
Primer sequence for the gene of interest and housekeeping genes.

Gene	Primer pairs
BAX	Fwd: 5′GGTGAACTGGGGGAGGATTG3′ Rev: 5′AGAGCGATGTTGTCCACCAG3′
Bcl_2	Fwd: 5′GGTGAACTGGGGGAGGATTG3′ Rev: 5′AGAGCGATGTTGTCCACCAG3′
Caspase-3	Fwd: 5′GGAGCTTGGAACGCGAAGA3′ Rev: 5′ACACAAGCCCATTTCAGGGT3′
Claudin-5	Fwd: 5′CGAGGCAAGTTAGGTTGGGT3′ Rev: 5′GGTCGGTCAAGTCCTCACAA3′
Occludin	Fwd: 5′TTCTGTGCTCACAGGTGGTT3′ Rev: 5′TGGGCTGGATGCCAATTTAGT3′
INSR	Fwd: 5′TGTGACTGATTATTTAGATGTCCCA3′ Rev: 5′CATCTGGCTGCCTCTTCCTC3′
IRS-1	Fwd: 5′CTGCATAATCGGGCAAAGGC' Rev: 5′GCCCGTGTCATAGCTCAAGT3′
GAPDH Housekeeping	Fwd: 5′AAGAAGGTGGTGAAGCA GG3′ Rev:5′CAAAGGTGGAAGAATGG GAG3′
ACTB Housekeeping	Fwd: 5′AACCTTCTTGCAGCTCCTC3′ Rev: 5′ACCCATACCCACCATCAC AC3′

2.6. Histomorphometry using Giemsa stain and immunohistochemistry for neurogenesis

Each brain hemisphere per animal (in each treatment group) was placed in sucrose overnight and mounted on a freezing microtome with dry ice and sucrose and cut in the sagittal plane at 50 μm. Six brain sections were serially collected (36 sections per group) at 300 μm apart, between Bregma plate 169 to plate 177 corresponding to the rat brain atlas [52]. The first series of sections were stained with Giemsa solution (Sigma-Aldrich, Product number 1.09204.00) made up in potassium dihydrogen phosphate (pH 4.5) for neuronal histomorphology, while the next two series of sections were used for immunohistochemical labelling of Ki67 and DCX, respectively.

2.6.1. Neuronal number and nuclei area

Within each Giemsa-stained section, nine camera fields were captured at X1000 magnification from uniformly selected areas of the hippocampal regions. Two camera fields each were captured within the CA1 and CA3 regions respectively while five camera fields were captured from the dentate gyrus (DG) region; two from each arm and one from the apex of the dentate gyrus giving a total of three hundred and twenty-four camera fields per group that was analysed. The number of neurons and nuclei area in the upper focal plane of these camera fields were determined using the cell counter and trace plugins of ImageJ software respectively. Only neurons with a vesicular nucleus and centrally placed nucleoli were measured and counted. Representative photomicrographs were compiled using Microsoft Visio and no manipulation was made to the captured images except for brightness and contrast.

2.6.2. Volume of the dentate gyrus

Photomicrographs of the Giemsa-stained dorsal hippocampus of each brain section was obtained using a Leica ICC50 HD video camera linked to a Leica DM 500 microscope (Leica Biosystems, USA). Within each section, the entire dorsal hippocampus was captured at X25 magnification, all 6 camera fields per group were imported in a stacked sequence, and the image j Volumest plugin was used in quantifying the volume of the granular layer and molecular layer in the dentate gyrus of each animal per group. The Volumest plugin entails a combination of the grid and Cavalieri's principle obtained by tracing out the region of interest for each of these layers in each camera field of an image sequence and the estimated volume for each layer was obtained in mm^3.

2.6.3. Immunohistochemistry for neurogenesis

From each brain hemisphere, six sections between plates 172–177 were selected using the atlas of the rat brain [52] for each histochemical

labelling. Free-floating brain sections in 24 well plates first underwent endogenous peroxidase inhibition with 50% methanol, 50% PB, and 1.66% hydrogen peroxide. Sections were washed, then blocked in 3% normal goat serum, 2% (BSA), and 0.25% Triton x 100 in 0.1 M PB for 2hrs at room temperature, followed by incubation in the primary antibodies (rabbit polyclonal antibody; Abcam, Cambridge, MA, USA), Ki67 and DCX (Abcam, USA; AB15580 and AB18723 respectively) with dilution factors 1:1000 and 1:3000 respectively for 48 hrs. The sections were washed with 0.1PB and incubated for 2 hr with secondary antibody (goat anti-rabbit antibody IgGs; Vectastain, Burlingame, CA USA). Washed and incubated for 1 hr with ABC kit (Vectastain, Burlingame, CA USA) and stained with DAB, mounted on gelatine-coated slides, dehydrated, and cleared in xylene. Control sections were incubated in 0.1MPB omitting the primary antibody. Photomicrographs of Ki67 and DCX immunolocalized dorsal hippocampus brain sections were obtained and counts of immunolabelled cells were determined by the cell counter plugin of Image J. Only DCX cells in the upper focal plane with a pale centrally placed centre were counted while immunolocalized cells for Ki67 were counted in clusters.

2.7. Statistical analysis

The diabetic parameters, number, and nuclei area of neurons in hippocampal regions, concentrations of cytokines and oxidative markers, expression of hippocampal Ki67 and DCX labelling as well as gene expression mRNA levels of insulin receptors, junctional and apoptotic genes were recorded as mean ± SEM. The data were subjected to a normality test using the Shapiro-Wilks test, parametric data were analysed using a one-way ANOVA test and a Post hoc Bonferroni's test was conducted to determine the difference between the groups. Nonparametric data were analysed by the Kruskal Wallis test and a Post hoc Duncan's pairwise analysis. The results with $P < 0.05$ were regarded as significant. All data analysis was carried out using the IBM SPSS statistics version 28.

2.8. Ethical clearance

This study was approved by the Animal Research Ethics Committee (approval number 2018/011/58/C) of the University of the Witwatersrand. All experimental animal handling and treatments were carried out according to the standards and principles set forth by this committee.

3. Results

3.1. Food, fluid consumption, and blood glucose across experimental groups

A decrease in food intake across treated groups was observed with a significant reduction in AL, AA, DAL, and DAA compared to the control (Fig. 1A). The diabetic groups consumed more fluid compared to the other groups with a significant increase in water consumption in DB and

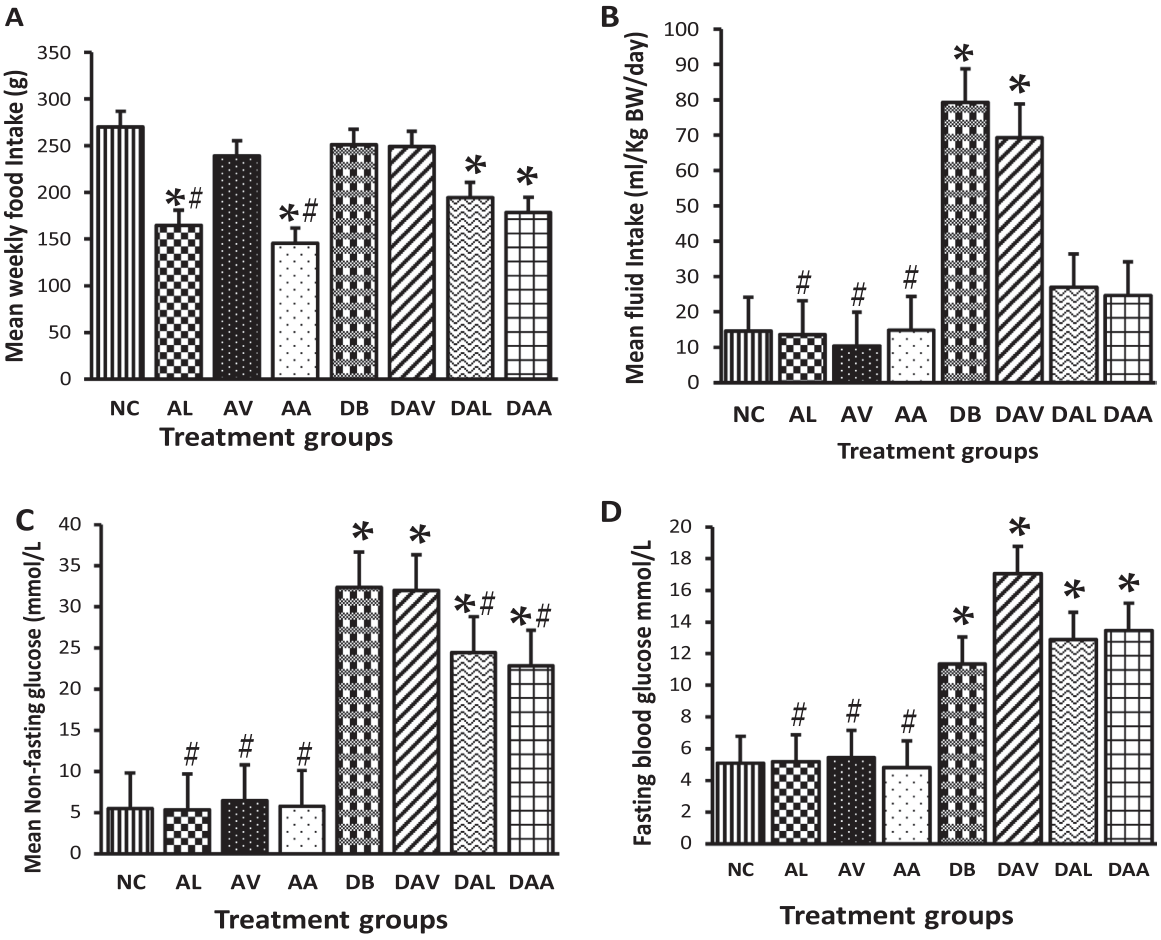

Fig. 1. Mean food and fluid intake, non-fasting, and fasting blood glucose across groups. A) Significant difference in mean food intake between groups (One way ANOVA $P = 0.001$). B) Significant difference in mean fluid intake between groups (Kruskal Wallis test, $P = 0.001$). C, D) Significant difference in mean random NFBG and FBG (One way ANOVA $P > 0.001$). $n = 6$ '*' significantly different compared to control, '#' significantly different compared to diabetes $P \leq 0.05$. NC: Control, AV: cART, AL: alcohol, AA: cART and alcohol, DB: diabetic, DAV: diabetic and cART, DAL: diabetic and alcohol, DAA diabetic cART and alcohol.

DAV compared to the other groups. No significant difference in fluid intake was observed between the AL, AV, and AA groups (Fig. 1B). The mean non-fasting blood glucose of the diabetic groups was significantly increased ($P < 0.05$) compared to the control (NC) and non-diabetic treated groups (AL, AV, and AA). The highest mean NFBG was observed in the DB group followed by the DAV, DAA, and DAL groups respectively (Fig. 1C). The mean FBG of the diabetic groups was significantly higher compared to the control and all other non-diabetic treated groups (Fig. 1D).

3.2. Oral glucose tolerance test and AUC of treated groups

The mean area under the OGTT curve (AUC) was significantly increased in the DB, DAV, DAL, and DAA groups compared to the control, AL, AV, and AA groups, also the AUC level in the DAV is significantly elevated compared to the DAL and DAA (Fig. 2A). The mean OGTT was similar with uniform low levels of blood glucose for the non-diabetic treated groups at different time intervals, while the diabetic groups (DB, DAV, DAL, and DAA) all had marginal erratic high glucose levels; at fasting, 30 min and 1 h post glucose load the diabetic groups maintained similar parallel levels of blood glucose increase with DAL slightly above DAA at fasting and 1 h post glucose load. At 2 h post glucose load; the DAV group maintained the highest blood glucose level while the DAL dropped to the lowest level for the diabetic groups at 18,5 mmol/L (Fig. 2B).

3.3. Mean insulin receptor genes expression in hippocampal tissue

The expression of INSR mRNA in the hippocampal homogenate was significantly downregulated in the AA and DB groups compared to the control ($P = 0.020$ and 0.023), AL ($P = 0.01$), AV ($P = 0.018$ and 0.028), and DAL ($P = 0.016$ and 0.043), while DAV and DAA are downregulated compared to DAL ($P = 0.01$; Fig. 2 C). Similarly, IRS-1 mRNA expression in the AL, AV, AA, DB, and DAV are significantly down-regulated compared to control ($P = 0.001$, 0.001, 0.001, 0.001, and 0.008), DAL ($P = 0.028$, 0.05, 0.001, 0.004 and 0.002), and DAA ($P = 0.05$, 0.05, 0.01, 0.01, 0.021 and 0.028; Fig. 2D). Conversely, the expression of IRS1 in the DAL and DAA groups was upregulated, significantly in the DAL group compared to the control.

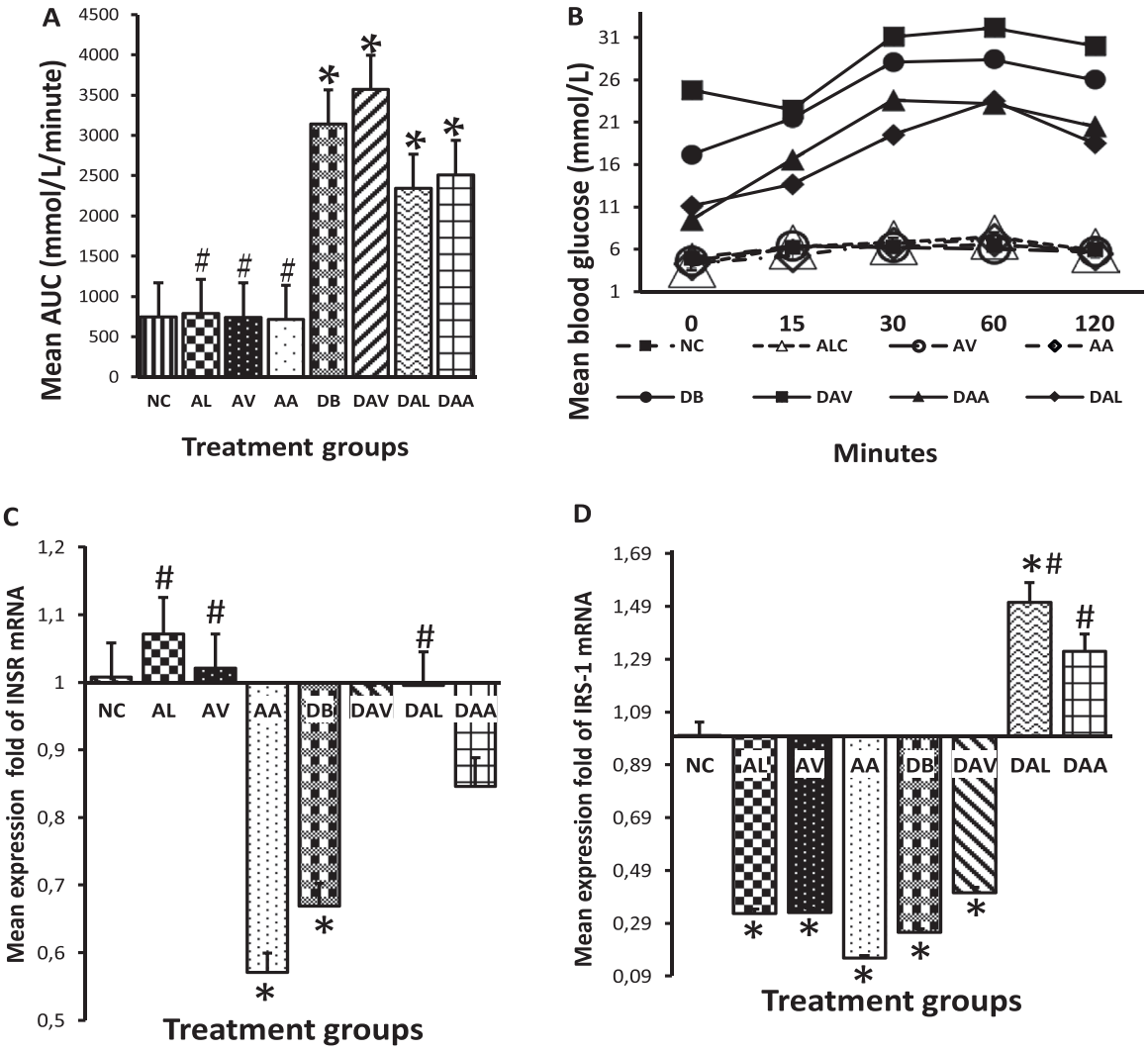

Fig. 2. Mean terminal Area under the curve (AUC), oral glucose tolerance test (OGTT), mRNA expression of insulin receptors (INSR and IRS-1) in hippocampal tissue. across groups. A) Significant difference in mean terminal AUC (One way ANOVA $P = 0.001$). '*' significantly different compared to control, '#' significantly different compared to diabetes ($P = 0.05$, Bonferroni post hoc test). B) Mean OGTT at different time intervals, DAV with highest values. C) Significant difference in insulin receptor mRNA expression (Kruskal Wallis, $P = 0.05$). D) Significant difference in insulin receptor substrate mRNA expression (Kruskal Wallis, $P = 0.007$). '*' significantly different compared to control, '#' significantly different compared to diabetes $P \leq 0.05$ $n = 3$. Key: NC: Control, AV: cART, AL: alcohol, AA: cART and alcohol, DB: diabetic, DAV: diabetic and cART, DAL: diabetic and alcohol, DAA diabetic cART and alcohol.

3.4. Proinflammatory cytokines and oxidative stress markers

The mean concentrations of proinflammatory cytokines across all the experimental groups are reported in Table 2. The concentration of IL-6 is significantly elevated in the AL, AV, and DAA groups compared to the control and AA groups. The concentration level of TNFα is significantly elevated in AL and AV groups compared to the control. While the concentration level of IL-1α is significantly elevated in the AL and DAA groups compared to the control and AA groups. Furthermore, the concentration of IL-1α, IL-6, and TNFα in DB and DAV groups reduced significantly against the control and all other treated groups but no significant difference occurs between cytokine levels in DB and DAV groups (Table 2). The lipid peroxidation levels recorded are significantly increased in all the experimental groups (AL, AV, DB, DAV, DAL, and DAA) in comparison to the control except for the AA group. However, MDA levels in the AL and DAV group were significantly increased compared to the AA group. Also, the antioxidant (GP_X) level was significantly reduced in all the experimental groups (AL, AV, AA, DB, DAV, DAL, and DAA) relative to the control and significantly reduced in the AA, DB, DAV, and DAL groups compared to AL and DAA groups (Table 2).

3.5. Mean expression of membrane-associated junctional proteins in the hippocampal tissue

The analysis of claudin-5 and occludin expression levels in the hippocampus reveals mostly the downregulation of these junctional proteins across the experimental groups (Fig. 3 A-B). Claudin-5 was observed to be significantly downregulated in the AA, AV, DB, and DAV groups compared to the control (P = 0.031, 0.004, 0.034, and 0.043) but downregulated in the AV group compared to the AL, DB, DAV, DAL, and DAA groups (P = 0.004, 0.015, 0.007, 0.001, 0.027; Fig. 3A). Occludin was significantly downregulated in the DAA group compared to the control (P = 0.045) and also downregulated in the AA and DB groups compared to the control (P = 0.023, 0.017), AV (P = 0.003, 0.001) and DAL groups (P = 0.025 and 0.002; Fig. 3 B).

3.6. Mean fold expression of apoptotic genes in hippocampal tissue

The mRNA expression of the three major apoptotic markers is shown in Fig. 3 with significant up up-regulation of Bcl_2 in the DAL, and DAA groups compared to the control (P = 0.045, and 0.029 respectively), and compared to the DB (P = 0.001) and DAV groups (P = 0.018 and 0.015). Conversely, Bcl_2 mRNA expression in the AA group is downregulated compared to control, AL, AV, DAL, and DAA (P = 0.03, 0.039, 0.023, 0.015, and 0.001 respectively, Fig. 4A). For BAX, a significant up-regulation was observed in the DAL compared to the control, AL, and DB groups (P = 0.001) and upregulated in the AL, DB, DAV, and DAA groups compared to the control (P = 0.01) and AV groups (P = 0.001). Similarly, BAX mRNA expression in the AA group is downregulated compared to control, AL, AV, DB, DAV, DAL, and DAA (P = 0.032, 0.014, 0.05, 0.031, 0.048, 0.001, 0.04 respectively, Fig. 4B). Caspase-3 in DB, DAV, DAL, and DAA was significantly upregulated against the control (P = 0.037, 0.001, 0.020, and 0.036) and AA (P = 0.032, 0.001, 0.017, and 0.031); and significantly upregulated in DAV compared to AL and AV treated groups (P = 0.009 and 0.003, Fig. 4C). The ratio of BAX to Bcl_2 reveal increased fold expression of BAX mRNA compared to Bcl_2 in the AL, DB, DAV, DAL and DAA, a reduced ratio in the AV and uniform levels in the AA group (Fig. 4D).

3.7. Mean number of neurons in different hippocampal regions

The estimated number of neurons in different hippocampal regions was significantly reduced, mostly in the diabetic groups (DB, DAV, DAL, and DAA) compared to other groups (Figs. 5–7). In the CA1 region, a uniform row of principal cells (circle, Fig. 5) and few peripheral glial cells (black arrows, Fig. 5) are seen in the NC group, followed closely by the AA, and AV groups. The CA1 neuronal number (CA1N) in the DAV, DAL, and DAA are significantly reduced compared to control, AL, AV, AA, and DB (P = 0.001). AL and DB are significantly decreased compared to control (P = 0.007 and 0.004; Fig. 5A) with a thin row of neurons, of which some present pyknotic nuclei (red arrows, Fig. 5) observed especially in the DAA group. In the CA3 region, a cluster of uniformly sized cell neurons with few glial cell nuclei are observed in the control group, and slightly similar histology was observed in the AA, and AV groups (Fig. 6). There number of neurons in the CA3 (CA3N) is significantly reduced in the DAV and DAL are significantly reduced compared to control (P = 0.001), AV (P = 0.016 and 0.005) and AA (P = 0.001), while DAA is significantly reduced compared to control, AL, AV, AA, and DB (P = 0.001, 0.013, 0.001, 0.001 and 0.019; Fig. 6A, P < 0.05). Additionally, the neurons in the diabetic comorbidity groups (DAV, DAL, and DAA) appeared dispersed and diffused with few cells pyknotic (red arrows, Fig. 6). In the DG region, a wide and dense layer of granular cell neurons are observed in the control group (Fig. 7) with a significant reduction in neuronal number in all the experimental groups compared to the control (P < 0.05, Fig. 7A). The AL, AV, AA, DB, and DAA are significantly reduced compared to control (P = 0.001). DAL is significantly decreased compared to control and AV (P = 0.001 and 0.003). The DAV group is the most severely affected with significantly reduced DG neuronal number relative to the control, AL, AV, AA, and DAA groups (P = 0.001, 0.033, 0.001, 0.004, and 0.044 respectively; Fig. 8A), followed by the DAL with fewer granular neurons (Fig. 7).

3.8. Mean neuronal nuclei in different hippocampal regions

The neuronal nuclei area at all hippocampal regions (CA1, CA3, and DG) are significantly increased in the DB group compared to the control (NC), AV, DAV, DAL, and DAA groups (P = 0.05, Fig. 5 A,6 A, and 7 A),

Table 2
Mean concentration of cytokines IL-1α, IL-6, TNFα, and oxidative stress markers MDA and GPx in hippocampal tissue homogenate.

	IL-6 (pg/ mg protein)		TNF-α (pg/ mg protein)		IL-1α (pg/ mg protein)		GPx (pg/ mg protein)		MDA (μmol/g protein)	
	Mean	Std Err	Mean	Std Err	Mean	Std Err	Mean	Std Err	Mean	Std Err
NC	1.507	0.02	1.187	0.05	3.349	0.09	2.165	0.08	0.032	0.001
AL	1.888	0.10*#	1.429	0.04*#	3.982	0.2*#	1.505	0.09*#	0.077	0.002*
AV	1.840	0.05*#	1.333	0.03*#	3.774	0.15*#	1.278	0.01*	0.069	0.002*
AA	1.517	0.05#	1.098	0.03#	3.132	0.22#	1.186	0.01*	0.044	0.002
DB	1.104	0.01*	0.826	0.03*	2.455	0.01*	1.193	0.05*	0.065	0.006*
DAV	0.981	0.07*	0.847	0.01*	2.527	0.22*	1.187	0.04*	0.083	0.011*
DAL	1.780	0.11#	1.260	0.12#	3.908	0.13#	1.116	0.01*	0.066	0.004*
DAA	2.008	0.09*#	1.272	0.01#	4.035	0.12*#	1.476	0.10*#	0.061	0.002*

Data reported as mean ± SEM. Significant difference in the mean concentration of cytokines (IL-1α, IL-6, TNFα), MDA, and GPX between groups (One way ANOVA P = 0.001). '*' is significantly different compared to the control, and '#' is significantly different compared to diabetes P ≤ 0.05. n = 4. Key: NC: Control, AV: cART, AL: alcohol, AA: cART and alcohol, DB: diabetic, DAV: diabetic and cART, DAL: diabetic and alcohol, DAA diabetic cART and alcohol.

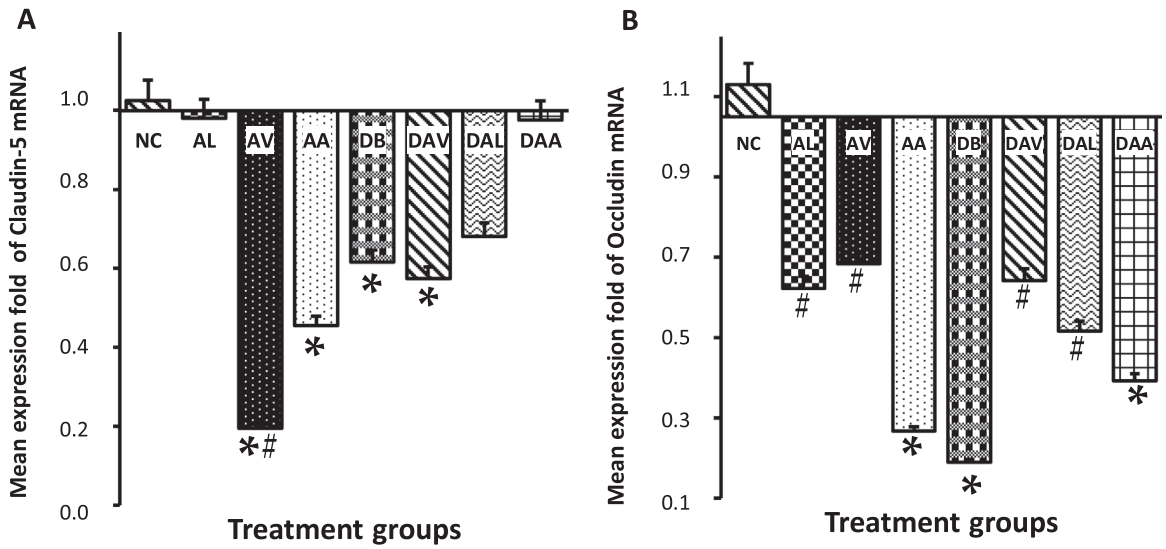

Fig. 3. Mean mRNA expression of membrane-associated junctions (claudin-5 and occludin) in hippocampal tissue. A) Significant difference in claudin-5 expression (One-way ANOVA, P = 0.013). B) Significant difference in occludin expression (One-way ANOVA, P = 0.05). '*' significantly different compared to control, '#' significantly different compared to diabetes P ≤ 0.05, n = 3. Key: NC: Control, AV: cART, AL: alcohol, AA: cART and alcohol, DB: diabetic, DAV: diabetic and cART, DAL: diabetic and alcohol, DAA diabetic cART and alcohol.

with observed enlarged nuclei in neurons at all the hippocampal regions of the DB groups (circles, Figs. 5–7). In the AL group, neuronal nuclei area significantly increased compared to the control, AV, DAV, DAL, and DAA groups at the CA1 and DG regions (P = 0.05, Figs. 5B and 7B). Additionally, neuronal nuclei area in the AA group is significantly increased in the CA1 region (compared to control and DAA groups) and in the DG region (compared to AV, DAL, and DAA) (P = 0.05, Figs. 5B and 7B). These increased neuronal nuclei area in the AL and AA were observed as large round and vesicular nuclei which form a slightly wider layer of cells despite the decreased number of neurons, especially in the AL group (circles, Figs. 5 and 7). Furthermore, the neurons in the diabetic groups (DAV, DAL, and DAA) appear diffuse and irregularly shaped, especially in the DG of the DAL group and in the CA1 and CA3 region of the DAV group with a dark and pyknotic appearance (red arrows, Figs. 5 to 7).

3.9. Mean volume of the granular and molecular layer in the dentate gyrus

A reduction in the molecular layer (ml; black double arrows, Fig. 8) and granular layer (GL; double red arrows, Fig. 8) of the dentate gyrus in all the treated groups is evident in low-power microscopy, especially in the DAV and DAL groups (Fig. 8). The volume of the granular cell layer in the dentate gyrus is significantly reduced in the AA, DAL, DAV and DAA compared to control (Fig. 8A, P = 0.05) and significantly decreased in the AA and DAL groups compared to DB group (Fig. 8A, P = 0.05). A significant reduction in the molecular layer volume of the diabetic groups (DB, DAV, DAL, and DAA) compared to the control was observed, with further reduction in the DAL, and DAA groups compared to the AV group (Fig. 8B; P = 0.05).

3.10. Immunohistochemical expression of hippocampal double courtin

In the control group, several areas of DCX immunolabelling clusters are observed (black arrows, Fig. 9), and closely similar observations are made in the AV and AA groups. Few DCX-expressing neurons were detected in the DB and DAA groups with further minimal expression in the AL, DAV, and DAL groups (black arrows, Fig. 9). The apex of the dentate gurus captured at higher magnification and reveal DCX expression in neuronal cell bodies and processes of the control AV, and AA groups, while the DCX expression was observed in the AL was mostly in the processes (arrowheads; Fig. 9). Waning DCX expression was observed in the DB group followed by the DAA and then DAV groups (arrowheads; Fig. 9), and no expression was observed in this camera field of the DAL group.

Quantification of immunolabelled cell bodies reveals that the AL, DB, and DAA treated groups contained significantly less DCX expressing neurons compared to the control (P = 0.001), AV (P = 0.001), and AA (P = 0.024, 0.001 and 0.001; Fig. 9A), while the DAV and DAL groups expressed significantly less DCX compared to all other groups except in comparison each other (P = 0.001 and 0.11, Fig. 9A), but DCX expression levels in AV and AA was not significantly affected.

3.11. Immunohistochemical expression of hippocampal Ki67

The immunohistochemical labelling of Ki67 clusters in the dentate gyrus reveals several areas are immunoreactive for Ki67 (black arrows, Fig. 10) in the control group, which is slightly similar to the AV group. Areas expressing Ki67 are reduced in other experimental groups with the most minimal Ki67 expression in the DAL and DAA groups. The apex of the dentate gyrus (squares, Fig. 10) is captured at higher magnification and shows multiple Ki67 expressed clusters in the control group, and individual clusters in other treated groups (circles, Fig. 10) except the AL, DAV, and DAL group where no Ki67 expression was observed in these camera fields. Quantification of Ki67 expression reveals significantly reduced Ki67 in AL, AA, DB, and DAA groups except compared to the control (P = 0.009, 0.010, 0.002, and 0.001 respectively). The DAL and DAV groups express significantly less Ki67 compared to the control (P = 0.001) and AV groups (P = 0.039 and 0.009; Fig. 10).

4. Discussion

The pathogenesis of cognitive disorders has been severally associated with hyperglycemia and hippocampal insulin resistance in diabetic patients and experimental animals [9,47]. The maintenance of a diabetic condition is defined by hyperglycemia and glucose tolerance which are well defined in the diabetic groups (DB, DAV, DAL, and DAA) with observations of significantly elevated FGT, NFGT, and AUC compared to the control and other alcohol-treated groups (AL, AA). Thirst as a symptom of diabetes was significantly elevated in the DB and DAV groups supported by the significantly elevated mean fluid volume intake and normal food consumption. However, the alcohol-treated groups

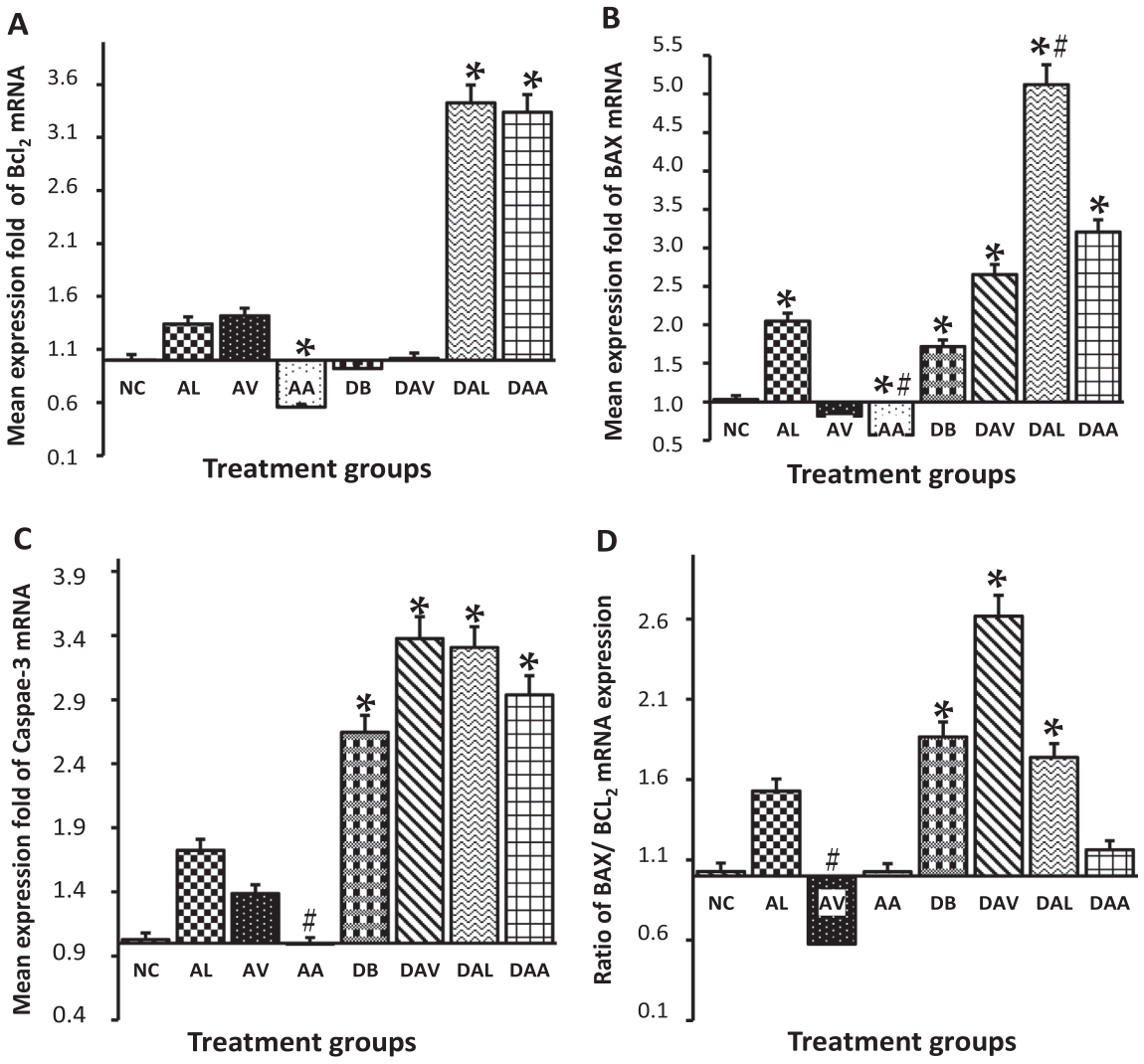

Fig. 4. Mean expression of membrane-associated junctions (claudin-5 and occludin) and apoptosis-associated genes (Bcl_2, BAX, and Caspase-3) in hippocampal tissue. Data presented as mean ± SEM. Significant difference in Bcl_2, BAX, and Caspase-3 expressions (One-way ANOVA, P = 0.007, 0.001, 0.006 respectively). A) For Bcl_2, AA is significantly downregulated while DAL and DAA are upregulated compared to the control ($P \leq 0.05$) B) For BAX, AA is significantly downregulated while DB, DAV, and DAL are significantly upregulated compared to the control ($P < 0.05$). C) For Caspase-3, DB, DAV, DAL, and DAA are significantly upregulated compared to control and AA ($P \leq 0.05$). D) The ratio of BAX to Bcl_2 is significantly greater in DB, DAV and DAL compared to the control ($P \leq 0.05$). '*' is significantly different compared to the control, and '#' significantly different compared to diabetes ($P \leq 0.05$, Bonferroni post hoc test). n = 3. Key: NC: Control, AV: cART, AL: alcohol, AA: cART and alcohol, DB: diabetic, DAV: diabetic and cART, DAL: diabetic and alcohol, DAA diabetic cART and alcohol.

(AL, AA, DAL, and DAA) consumed relatively lower amounts of food and fluid compared to the DB and DAV groups. This observation corroborates reports of reduced dietary intake with alcohol treatment in rats [41]. Hyperglycaemia in diabetes is often associated with neuronal deficits, especially in the hippocampal neurons (which are sensitive to insulin receptors) [9,34], low-grade inflammation or perturbation in pro-inflammatory cytokines and oxidative stress [20,55] which are inimical for cognitive functions.

Our results also clearly show the differential effects on hippocampal insulin receptors (IRS-1 and INSR) in the various treated groups with downregulation of IRS-1 in AL, AV, AA, DB, DAV treated groups but upregulated in the DAL and DAA groups, while INSR was downregulated in AA, DB, and DAA. This suggests that alcohol use (AL) and cART (AV) treatment may induce the depreciation of hippocampal insulin receptors which is implicated in the pathogenesis of T2D [40,66]. Similarly, the co-administration of alcohol and cART in the AA group further reduced insulin receptors which suggest impairment of hippocampal insulin utilization similar to effects reported in diabetes [4,29]. But the upregulation of insulin receptors in the DAL and DAA groups, and significantly lower NFBG levels in these groups compared to DB is consistent with earlier reports of mitigated glycaemic control and insulin sensitivity with alcohol use in diabetes [2,38]. These observations of impaired hippocampal insulin receptors are an indication of possible toxicosis and are often hallmarks of dysfunction in hippocampal cognition, behavioural despair, and anxiety-like behaviours [56,64,9].

The increased levels of inflammatory parameters (IL-1α, IL-6, and TNFα), and MDA with reduced GPX in the hippocampus of the AL and AV groups are also consistent with previous reports of alcohol and cART independent roles in neuroinflammation and oxidative stress [3,31,51,54]. However, concomitant alcohol use with cART (AA) ameliorated these independent effects of alcohol and cART on cytokines (IL-1α, IL-6, and TNFα) possibly due to synergistic interaction in the metabolism of alcohol and cART through cytochrome P enzyme pathways [42]. Interestingly, our result show for the first time that combined therapy of alcohol and cART (AA) in an HIV-naïve model reduces hippocampal MDA levels compared to control, however, the interaction in alcohol and cART (AA) also reduces GPX, and such antioxidant deficiency is implicated in the pathogenesis of diabetes [17]. In addition, significant

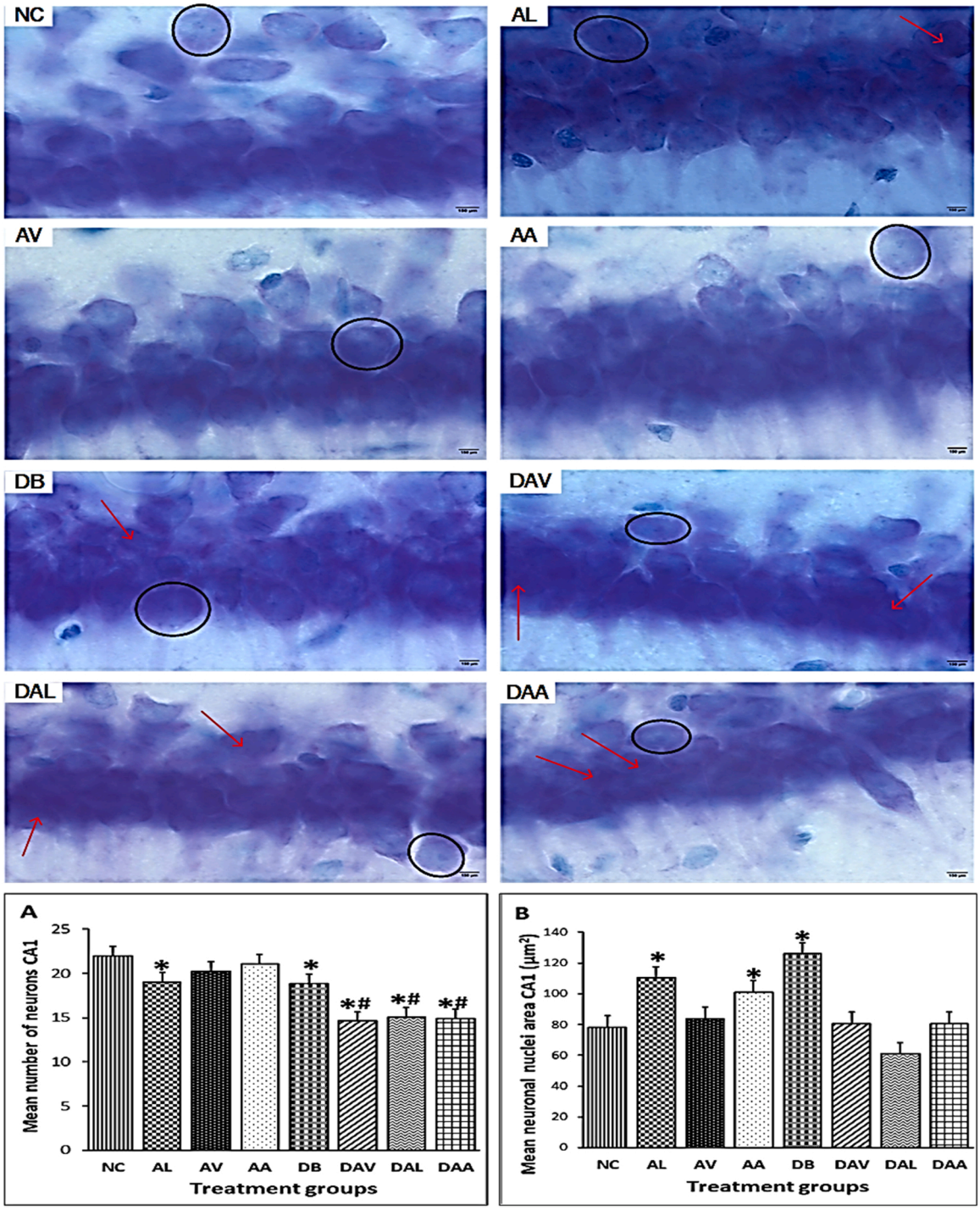

Fig. 5. Photomicrographs of the CA1 region in the dorsal hippocampus across different experimental groups. **A)** Significant difference between neuronal number at CA1 region across groups (One-way ANOVA, $P = 0.001$). **B)** Significant difference between neuronal nuclei area at CA1 region across groups (One-way ANOVA, $P = 0.001$). '*' is significantly different compared to the control, and '#' significantly different compared to diabetes ($P \leq 0.05$, Bonferroni post hoc tests). Circles indicate the area of neuronal nuclei, and red arrows indicate pyknotic nuclei of neurons. Scale bar 100 μm X1000. n = 6. Key: NC: Control, AV: cART, AL: alcohol, AA: cART and alcohol, DB: diabetic, DAV: diabetic and cART, DAL: diabetic and alcohol, DAA diabetic cART and alcohol.

deficiency of cytokines (IL-1α, IL-6, and TNFα) and the oxidative stress observed in the DB and DAV-treated groups could be an indicator of compromised immunometabolism and susceptibility to infection in diabetes [60,65], while neuroinflammation (elevated IL-1α and IL-6 levels) and oxidative stress observed with alcohol and cART combined-therapy in diabetes (DAA) may be due to influence of diabetes concomitantly with chemical injury of the treatment cumulating in metabolic complications and neuronal autophagy [72]. Furthermore, IL-6 can act both as a stimulator or inhibitor of insulin action in the pathogenesis of T2D [57,62] which corroborates with the observation of neuroinflammation (elevated IL-6 and INSR) in AL, AV but reduced IL-6, INSR and IRS-1 (anti-inflammatory) in DB and DAV treated groups in the advanced stages of diabetes [10,28].

Furthermore, insulin receptors (INSR and IRS-1) are expressed in neurons and endothelial cells of the blood-brain barrier (BBB) as required for cognitive and synaptic function [34,69] and have also been

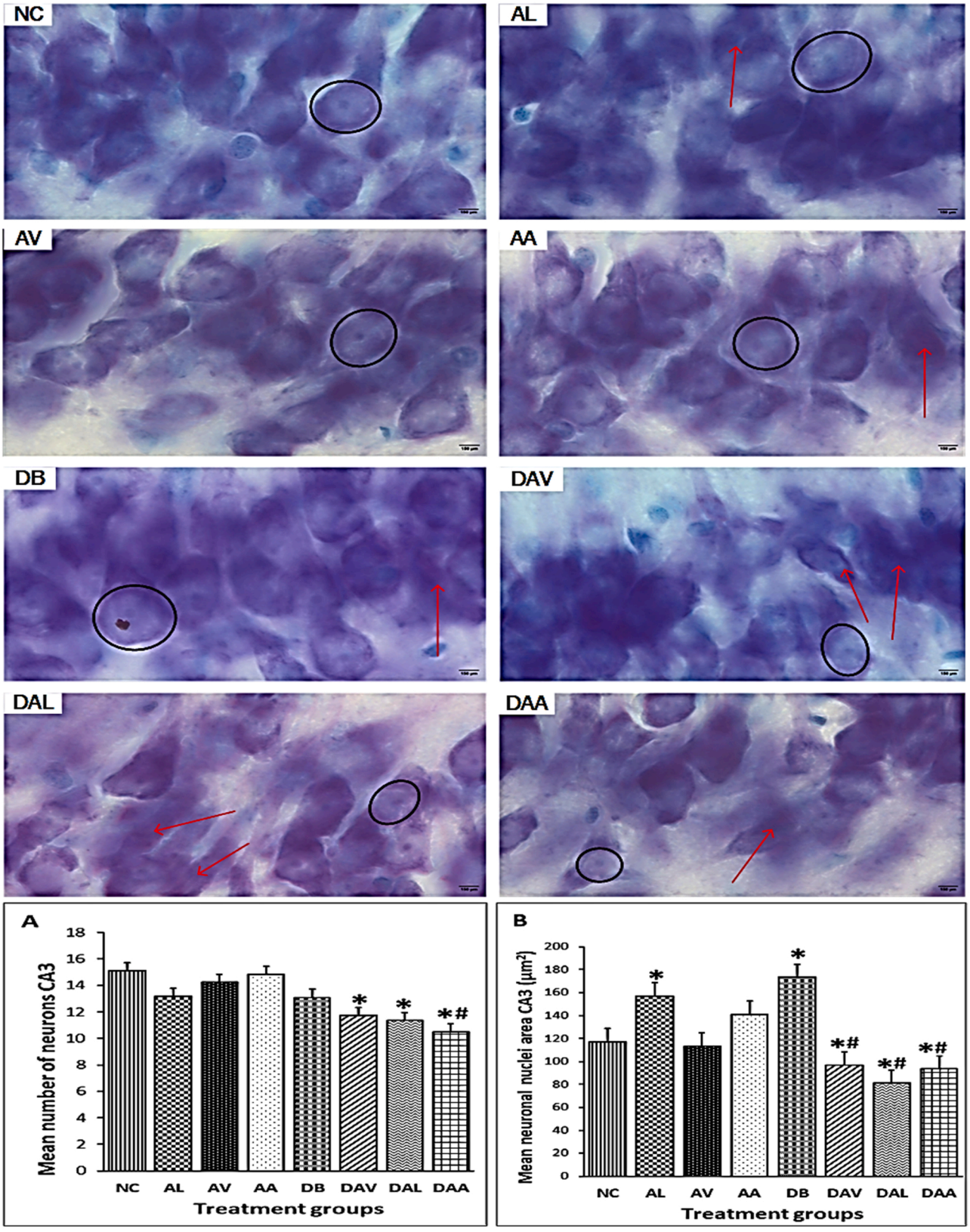

Fig. 6. Photomicrographs of the CA3 region in the dorsal hippocampus across different experimental groups. A) Significant difference in neuronal number across groups (One-way ANOVA, P = 0.001). B) Significant difference between neuronal nuclei area at CA1 region across groups (One-way ANOVA, P = 0.001). '*' is significantly different compared to the control, and '#' significantly different compared to diabetes ($P \leq 0.05$, Bonferroni post hoc tests). Circles indicate the area of neuronal nuclei and red arrows indicate pyknotic nuclei of neurons. Scale bar 100 μm X1000. n = 6. Key: NC: Control, AV: cART, AL: alcohol, AA: cART and alcohol, DB: diabetic, DAV: diabetic and cART, DAL: diabetic and alcohol, DAA diabetic cART and alcohol.

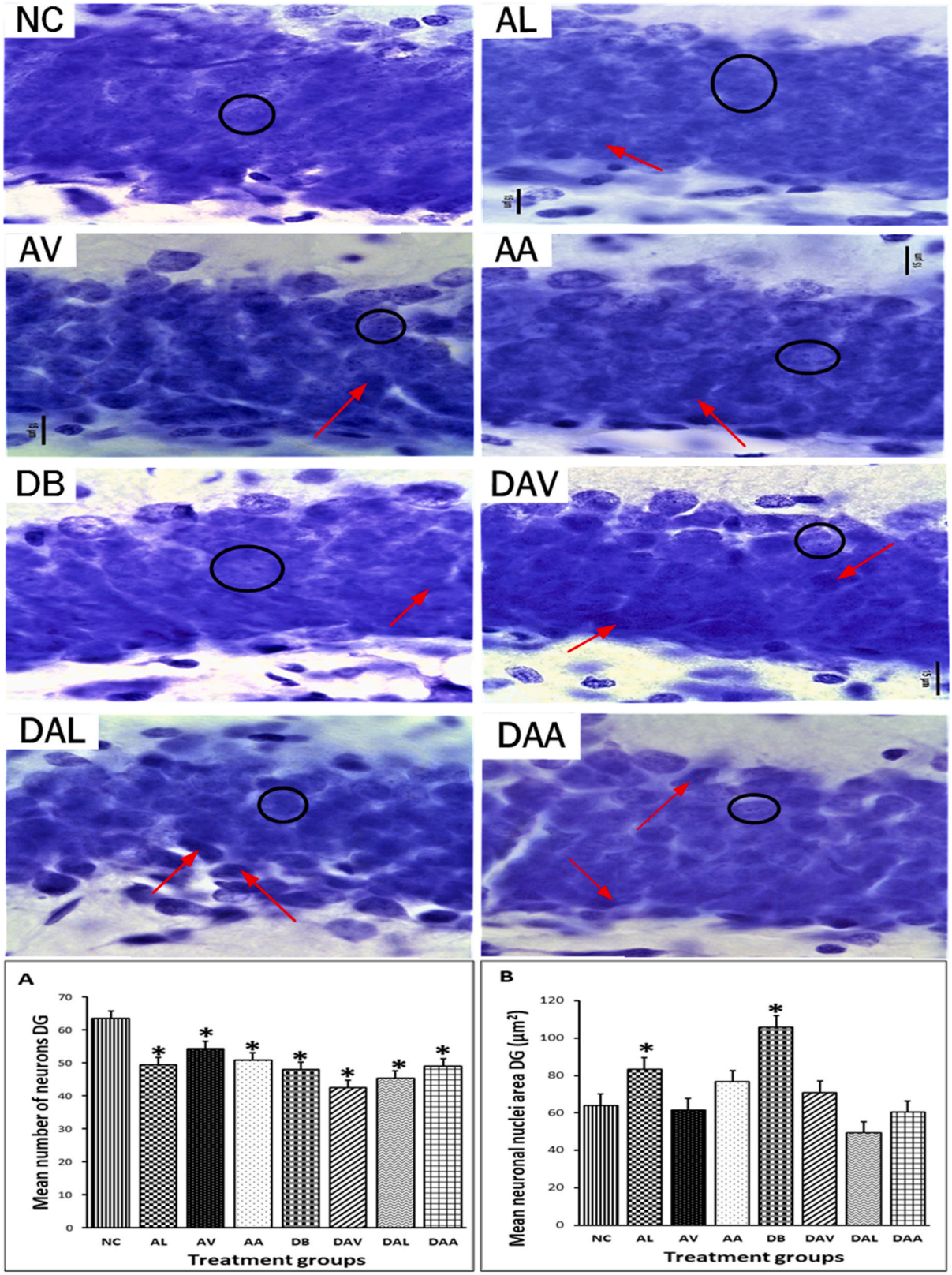

Fig. 7. Photomicrographs of the DG region in the dorsal hippocampus across different experimental groups. A) Significant difference between neuronal numbers across groups (One-way ANOVA, P = 0.001). B) Significant difference between neuronal nuclei area across groups (One-way ANOVA, P = 0.001). '*' is significantly different compared to the control, and '#' is significantly different compared to diabetes ($P \leq 0.05$, Bonferroni post hoc tests). Circles indicate the area of neuronal nuclei and red arrows indicate pyknotic nuclei of neurons. Scale bar 15 μm X1000. N = 6. Key: NC: Control, AV: cART, AL: alcohol, AA: cART and alcohol, DB: diabetic, DAV: diabetic and cART, DAL: diabetic and alcohol, DAA diabetic cART and alcohol.

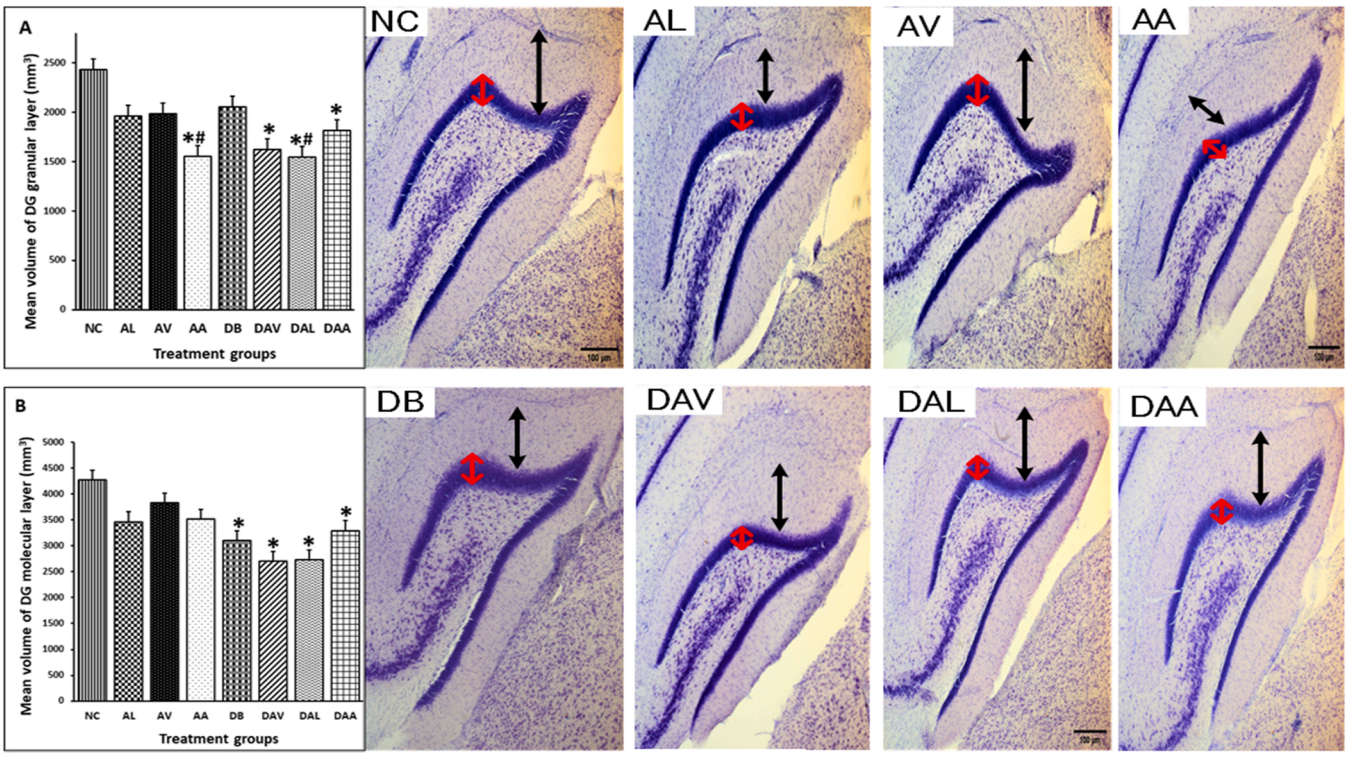

Fig. 8. Representative photomicrographs of dorsal hippocampus showing mean volume of granular (VDGGL) and molecular (VDGML) layers in the dentate gyrus of dorsal hippocampal sections. Significant difference in VDGGL and VDGML (Kruskal Wallis test P = 0.05 and 0.025 respectively). A) AA and DAL are significantly decreased compared to control (P = 0.018 and 0.026) and DB (P = 0.022 and 0.032), while DAV and DAA are significantly decreased compared to control (P = 0.05). B) DAL and DAA are significantly reduced compared to control (P = 0.002 and 0.007) and AV (P = 0.009 and 0.022), while DB and DAV are significantly decreased compared to control (P = 0.022 and 0.05). Molecular layer of the dentate gyrus (double black arrow); granular layer of the dentate gyrus (double red arrow). '*' significantly different compared to control, '#' significantly different compared to diabetes P ≤ 0.05. Scale bar 100 μm, X100. N = 6. Key: NC: Control, AV: cART, AL: alcohol, AA: cART and alcohol, DB: diabetic, DAV: diabetic and cART, DAL: diabetic and alcohol, DAA diabetic cART and alcohol.

implicated in the regulation of junctional proteins occludin and claudin-5 [49]. Thus, the significant downregulation of claudin-5 (AV, AA, DB, and DAV groups), and occludin in (AA, DB, and DAA groups) may be associated to the downregulation of insulin receptors in these groups which may indicate the potential of diabetes and /or cART-alcohol interaction to significantly increase BBB permeability. This could be due to the presence of Efavirenz, a component of cART, which impairs claudin-5 mRNA levels and increases BBB permeability irrespective of Efavirenz-induced cellular response that may not reveal corresponding claudin 5 protein expression, [7]. Vascular disruptions in diabetes may also independently induce BBB permeability [61]. Similarly, the impairment of BBB shown by non-significant downregulation of occludin and claudin-5 mRNA in the AL and DAL groups could be due to the ability of alcohol to cross the BBB.

This increased BBB permeability is associated with cellular pathology in cognitive impairment and apoptosis of hippocampal neurons [16, 35]. Therefore, observation of elevated apoptotic mRNA expressions (BAX and Caspase-3) in the DB, DAV, and DAA groups is indicative of apoptosis in these groups and suggests the potential of alcohol, diabetes, and/or cART to adversely affect hippocampal function. The potential effect of hippocampal apoptosis could be mitigated by the neurogenic niche of the dentate gyrus sub-granular zone. However, reduced expression of proliferating (Ki67) and immature (DCX) neurons in the alcohol (AL) and comorbidity groups (DB, DAV, DAL, and DAA), demonstrate impaired regenerative ability of hippocampus in these groups and consequently suggest impaired cognitive and memory activities previously reported in either alcohol, cART, and diabetes [33,48, 63]. Our results also demonstrate that cART exhibits a dual effect on neurogenesis, which is exacerbated in combination with diabetes (DAV) but is ameliorated when combined with alcohol (AA).

Histopathology investigations reveal two forms of cell death with morphological features of both necrosis and apoptosis, a condition of aponecrosis which supports our observations of mRNA expressions of BAX and Caspase-3. Features of necrosis such as increased neuronal nuclei size were observed in the AL, AA, and DB groups [27,37], while apoptosis and shrinkage of neuronal nuclei area [24,76] were observed in the diabetic comorbidity groups (DAV, DAL, and DAA). These nuclei morphology observations were further corroborated by a significant reduction of neuronal number in hippocampal regions, CA1 in (DB, DAV, DAL, and DAA groups), CA3 in (DAV, DAL, and DAA groups) and DG in all treated groups which agrees with the significant reduction in the volume of the dentate gyrus granular and molecular layer of the AA, DAV, DAL and DAA groups. The insignificant reduction in the volume of the dentate gyrus of the AL and DB group despite reduced neuronal number may be due to the necrotic enlargement of neuronal cells, presenting as a large volume. Furthermore, the significant reduction of DG neuronal number and antioxidant (GPx) level in all the treated groups highlights the venerability of the hippocampal dentate gyrus neurons to antioxidant deficiency induced by diabetes, alcohol, cART, and their combinatorial interactions. The DG has a unique neuronal network and interconnectivity through the hippocampal CA3 neurons [15,43] with other hippocampal regions and the chemical insult due to the treatment of the diabetic comorbidity groups (DAV, DAL, and DAA) may adversely affect its role in the integration of proliferating and immature neurons resulting in dysfunctional hippocampal neurogenesis.

Our results also reveals that the coadministration of alcohol and cART (without diabetes) in the AA group may potentially reduce hippocampal insulin receptors, antioxidants, antiapoptotic and BBB mRNA expression gene, cumulating in loss of DG neurons, proliferating neurogenic neurons and DG granular cell volume and neurogenesis.

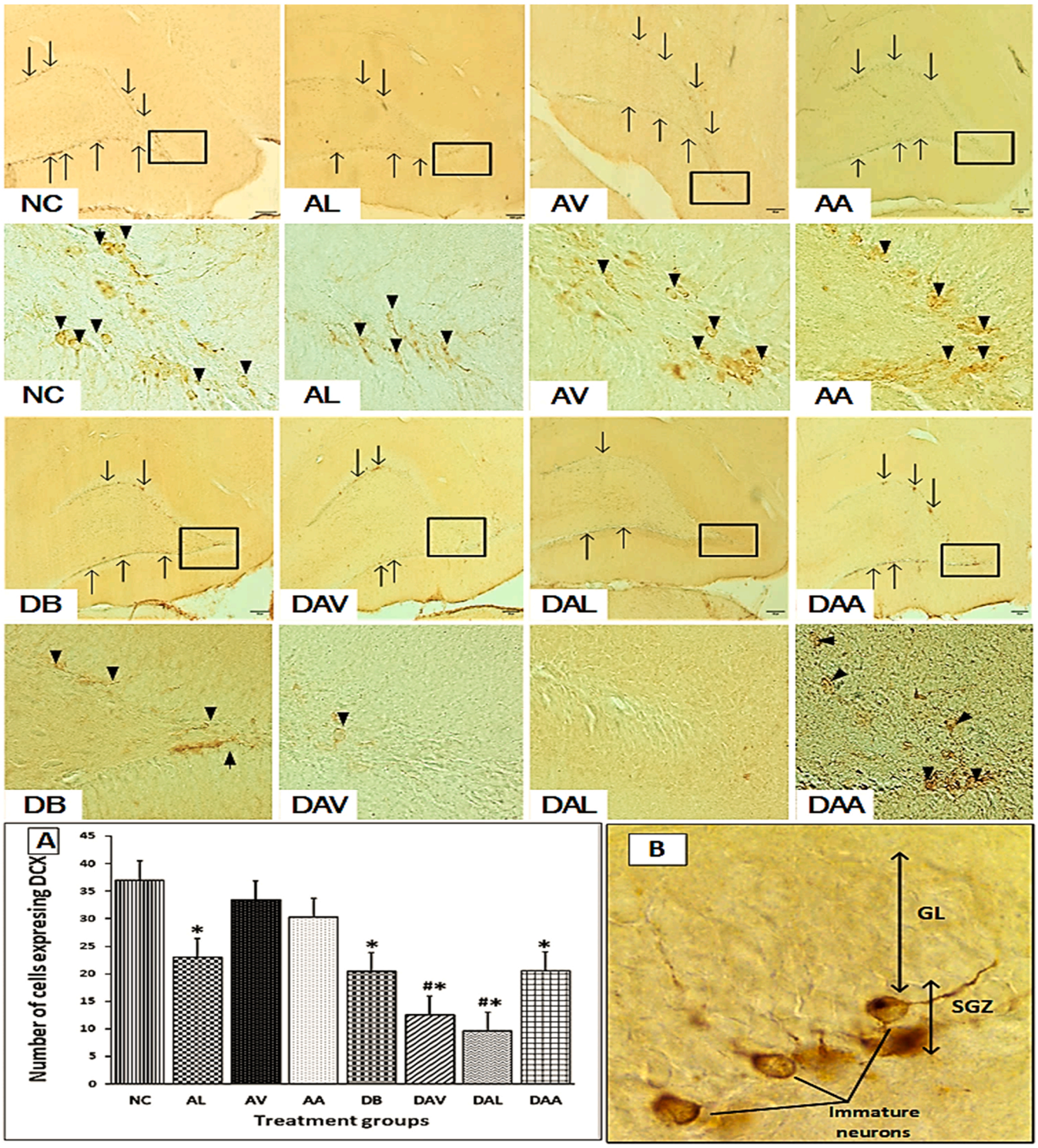

Fig. 9. Mean number of neurons expressing DCX and representative photomicrographs illustrating expression of DCX in the dentate gyrus region of the dorsal hippocampus. Arrows indicate areas of DCX expression, X50, scale bar 100 μm, squares indicate area captured at higher magnification X400, arrowheads indicate cell bodies of immature neurons expressing DCX. A) Significant difference in expression of DCX between groups (One Way ANOVA, $P = 0.001$). '*' is significantly different compared to the control, and '#' is significantly different compared to diabetes $P \leq 0.05$. **B)** A camera field of the dentate gyrus captured at higher magnification, illustrating the GL-granular cell layer, SGZ- sub-granular zone, and typical cell bodies of immature neurons quantified for DCX expression. X1000, scale bar 15 μm. $n = 6$, Key: NC: Control, AV: cART, AL: alcohol, AA: cART and alcohol, DB: diabetic, DAV: diabetic and cART, DAL: diabetic and alcohol, DAA diabetic cART and alcohol.

Thus, individuals exposed to AA treatment could potentially experience disrupted memory, and dentate gyrus-associated toxicosis. An earlier report indicated that dentate gyrus volume can significantly predict verbal learning and memory decline as previously reported [11]. Furthermore, these hippocampal effects observed in the AA group parallel effects observed in diabetes, which suggests that the chemo-toxic interaction in AA may induce dentate gyrus toxicosis similar to those observed in diabetes. Similarly, the interactive effects of T2D, alcohol,

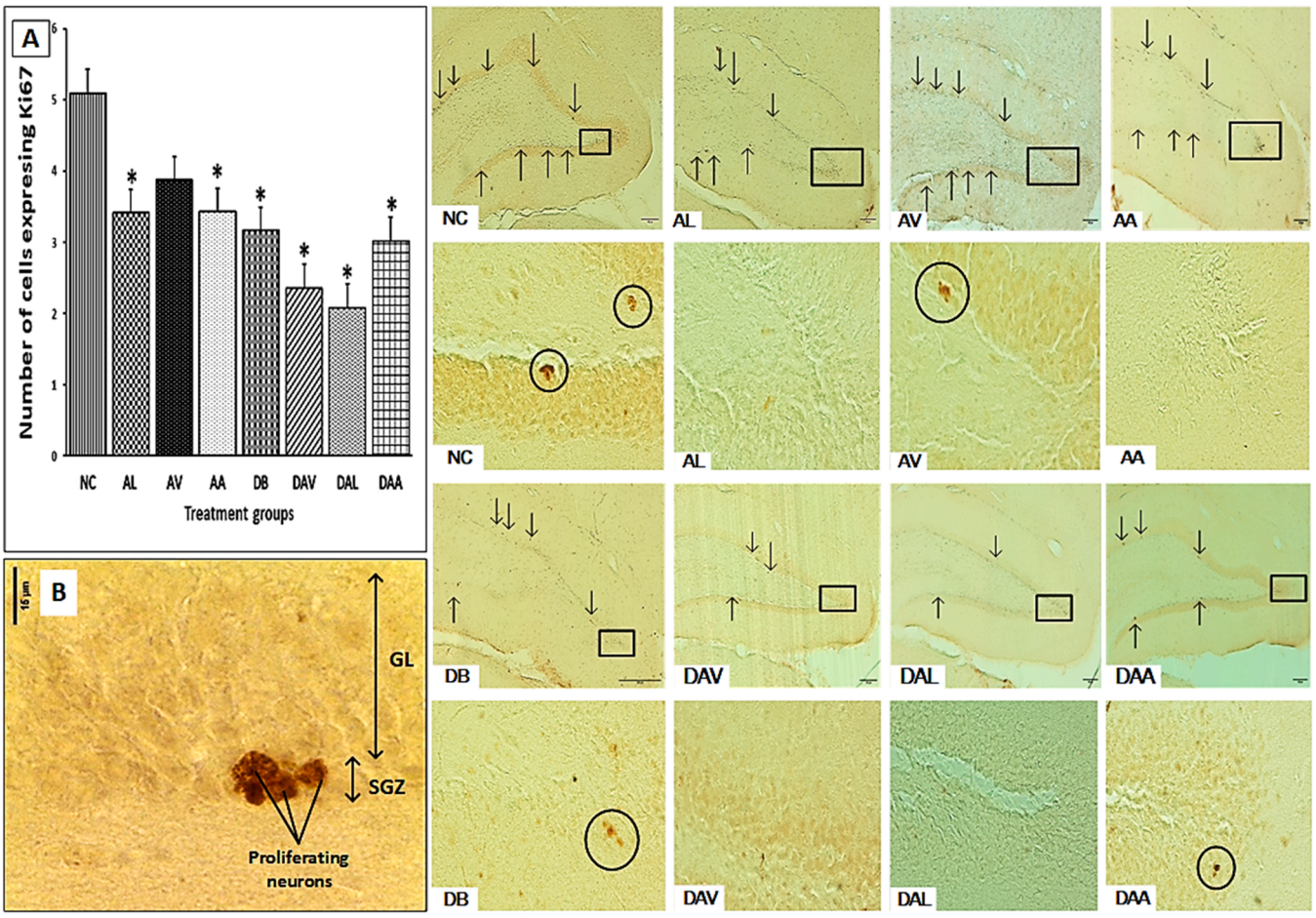

Fig. 10. Representative photomicrographs illustrating expression and mean number of neurons expressing Ki67 in the dentate gyrus region of the dorsal hippocampus. Arrows indicate areas of Ki67 expression, X50, scale bar 100 μm, square indicate area captured at higher magnification X400, circles indicate clusters of proliferating neurons expressing Ki67. A) Significant difference in expression of Ki67 between groups (One Way ANOVA, $P = 0.001$), '*' is significantly different compared to the control $P \leq 0.05$. B) A camera field of the dentate gyrus captured at higher magnification, illustrating the GL-granular cell layer, SGZ- sub-granular zone, and typical cell bodies of proliferating neurons quantified for Ki67 expression in a specific cluster. X1000, scale bar 15 μm. n = 6. Key: NC: Control, AV: cART, AL: alcohol, AA: cART and alcohol, DB: diabetic, DAV: diabetic and cART, DAL: diabetic and alcohol, DAA diabetic cART and alcohol. Arrows indicate areas of Ki67 expression, X50 scale bar 100 μm, and squares indicate area captured at higher magnification X400 scale bar 100 μm. Key: NC: Control, AV: cART, AL: alcohol, AA: cART and alcohol, DB: diabetic, DAV: diabetic and cART, DAL: diabetic and alcohol, DAA diabetic cART and alcohol.

and cART (DAA group) induce hippocampal effects similar to pathologies observed in diabetes alone with an additional hippocampal effects on neuroinflammation (IL-1α, and IL-6) which was not observed in the other diabetic groups. Though, the possible behavioural effects of this treatment regimen were not the focus of the present study, diabetic patients who receive cART and consume alcohol regularly may be susceptible to impaired hippocampus-dependent cognitive and contextual object discrimination memory function as previously reported in rodent studies with neuroinflammation [18,22].

5. Limitations

The limitations of the present study may include the limited number of samples used in analysis involving qPCR and Elisa techniques following the loss of some of the animals during the experiment. The gelatine route of administration mimicked the oral route recommended for the cART drug used, as against IP or IV routes. Additionally, a daily long term oral gavage administration of cART would be highly stressful to the animals and may become a source of confounding factors. Considering the multifaceted effects induced by diabetes, cART and alcohol on the hippocampus, further investigations into the cognitive and memory effects induced by this treatment should be considered. Additionally, this study reports on a systematic estimation of histopathological effect, but further studies would focus on automated stereology using a larger sample size to delineate the mechanism of changes that occur over time.

6. Conclusion

In conclusion the combination of diabetes, cART and alcohol induces a cascade of hyperglycemia, depleted insulin receptors, oxidative stress, perturbation of cytokine, and BBB disruption cumulate in hippocampal apoptosis with attendant hippocampal pathologies. The findings from this study can be clinically invaluable for diabetic individuals on cART prophylaxis who consume alcohol regularly, as several adverse hippocampal effects may become exacerbated with prolonged intake. Thus, assessment of hippocampal well-being in patients with these comorbidities and treatment combinations is invaluable.

Funding

This research was funded by the University of the Witwatersrand, Faculty of Health Sciences Faculty Research Committee Individual Grant awarded to Jaclyn Asouzu Johnson in 2019 and 2021 (grant number; 00125484211015121105000000000000000005254).

CRediT authorship contribution statement

Jaclyn Asouzu Johnson: Conceptualization, Methodology, Software, Data curation, Writing – original draft, Visualization, Investigation, Software, Validation, Writing – review & editing. **Rober Ndou**: Conceptualization, Resources, Supervision. **Ejikeme F Mbajiorgu**: Conceptualization, Methodology, Data curation, Writing – original draft preparation, Supervision, Validation, Writing – review & editing.

Declaration of Competing Interest

The authors declare that they have no known competing financial interests or personal relationships that could have appeared to influence the work reported in this paper.

Data Availability

Data will be made available on request.

Acknowledgments

Our appreciation goes to our co-workers, Eguavoen Idemudia and Vaughan Perry for their excellent collaborative efforts. And special appreciation goes to Mrs. Hasiena Ali for her technical and laboratory assistance.

Institutional review board statement

The study was conducted in accordance with the standards and principles set forth by the Wits Research Animal Facility (WRAF) (approval number 2018/011/58/C) of the University of the Witwatersrand.

References

[1] D. Accili, Can COVID-19 cause diabetes? Nat. Metab. 3 (2021) 123–125 (Available at), ⟨https://www.nature.com/articles/s42255-020-00339-7⟩.
[2] A.T. Ahmed, A.J. Karter, E.M. Warton, J.U. Doan, C.M. Weisner, The relationship between alcohol consumption and glycemic control among patients with diabetes: the kaiser permanente northern california diabetes registry, J. Gen. Intern. Med. 23 (2008) 275–282 (Available at), ⟨https://www.ncbi.nlm.nih.gov/pmc/articles/PMC2359478/⟩.
[3] C. Akay, et al., Antiretroviral drugs induce oxidative stress and neuronal damage in the central nervous system, J. Neurovirol. 20 (2014) 39–53.
[4] S.E. Arnold, Z. Arvanitakis, S.L. Macauley-Rambach, A.M. Koenig, H.-Y. Wang, R. S. Ahima, S. Craft, S. Gandy, C. Buettner, L.E. Stoeckel, D.M. Holtzman, D. M. Nathan, Brain insulin resistance in type 2 diabetes and Alzheimer disease: concepts and conundrums, Nat. Rev. Neurol. 14 (2018) 168–181.
[5] J. Asouzu Johnson, R. Ndou, E.F. Mbajiorgu, Combination Antiretroviral Therapy (cART) in diabetes exacerbates diabetogenic effects on hippocampal microstructure, neurogenesis and cytokine perturbation in male Sprague Dawley rats, Diagn. (2022). ⟨https://www.ncbi.nlm.nih.gov/pmc/articles/PMC9029837/⟩.
[6] A.D. Association, 2. Classification and diagnosis of diabetes, Diabetes Care 38 (2015) S8–S16.
[7] L. Bertrand, L. Dygert, M. Toborek, Antiretroviral treatment with efavirenz disrupts the blood-brain barrier integrity and increases stroke severity, Sci. Rep. 6 (2016) 39738.
[8] G.J. Biessels, F. Despa, Cognitive decline and dementia in diabetes: mechanisms and clinical implications, Nat. Rev. Endocrinol. 14 (2018) 591–604. ⟨https://www.ncbi.nlm.nih.gov/pmc/articles/PMC6397437/⟩.
[9] G.J. Biessels, L.P. Reagan, Hippocampal insulin resistance and cognitive dysfunction, Nat. Rev. Neurosci. 16 (2015) 660–671.
[10] A. Borsini, M.G. Di Benedetto, J. Giacobbe, C.M. Pariante, Pro- and Anti-Inflammatory properties of interleukin in vitro: relevance for major depression and human hippocampal neurogenesis, Int. J. Neuropsychopharmacol. 23 (2020) 738–750, https://doi.org/10.1093/ijnp/pyaa055. Accessed May 10, 2022.
[11] K.M. Broadhouse, L. Mowszowski, S. Duffy, I. Leung, N. Cross, M.J. Valenzuela, S. L. Naismith, Memory performance correlates of hippocampal subfield volume in mild cognitive impairment subtype, Front. Behav. Neurosci. (2019) 13. ⟨https://www.frontiersin.org/articles/10.3389/fnbeh.2019.00259⟩ [Accessed January 4, 2023].
[12] T.T. Brown, S.R. Cole, X. Li, L.A. Kingsley, F.J. Palella, S.A. Riddler, B.R. Visscher, J.B. Margolick, A.S. Dobs, Antiretroviral therapy and the prevalence and incidence of diabetes mellitus in the multicenter AIDS cohort study, Arch. Intern. Med. 165 (2005) 1179–1184.
[13] R.B. Camire, H.J. Beaulac, C.L. Willis, Transitory loss of glia and the subsequent modulation in inflammatory cytokines/chemokines regulate paracellular claudin-5 expression in endothelial cells, J. Neuroimmunol. 284 (2015) 57–66.
[14] S. Carlsson, N. Hammar, V. Grill, J. Kaprio, Alcohol consumption and the incidence of type 2 diabetes: a 20-year follow-up of the Finnish twin cohort study, Diabetes Care 26 (2003) 2785–2790.
[15] E. Cherubini, R. Miles, The CA3 region of the hippocampus: how is it? What is it for? How does it do it? Front. Cell Neurosci. 9 (2015) 19. ⟨https://www.ncbi.nlm.nih.gov/pmc/articles/PMC4318343/⟩.
[16] A. Chodobski, B.J. Zink, J. Szmydynger-Chodobska, Blood-brain barrier pathophysiology in traumatic brain injury, Transl. Stroke Res. 2 (2011) 492–516 (Available at), ⟨https://www.ncbi.nlm.nih.gov/pmc/articles/PMC3268209/⟩.
[17] M. Cyuńczyk, M.E. Zujko, J. Jamiołkowski, K. Zujko, M. Łapińska, M. Zalewska, M. Kondraciuk, A.M. Witkowska, K.A. Kamiński, Dietary total antioxidant capacity is inversely associated with prediabetes and insulin resistance in bialystok PLUS population, Antioxidants 11 (2022) 283.
[18] J. Czerniawski, T. Miyashita, G. Lewandowski, J.F. Guzowski, Systemic lipopolysaccharide administration impairs retrieval of context–object discrimination, but not spatial, memory: Evidence for selective disruption of specific hippocampus-dependent memory functions during acute neuroinflammation, Brain Behav. Immun. 44 (2015) 159–166. ⟨https://www.sciencedirect.com/science/article/pii/S088915911400467X⟩.
[19] R. Daneman, A. Prat, The blood–brain barrier, Cold Spring Harb. Perspect. Biol. 7 (2015) a020412.
[20] De Felice F.G., Ferreira S.T., 2014. Inflammation, Defective Insulin Signaling, and Mitochondrial Dysfunction as Common Molecular Denominators Connecting Type 2 Diabetes to Alzheimer Disease. Diabetes 63:2262–2272 Available at: https://doi.org/10.2337/db13–1954 [Accessed September 20, 2022].
[21] De Meyts P., 2000. The Insulin Receptor and Its Signal Transduction Network. In: Endotext (Feingold KR et al., eds). South Dartmouth (MA): MDText.com, Inc. Available at: http://www.ncbi.nlm.nih.gov/books/NBK378978/ [Accessed June 30, 2022].
[22] E.J. Donzis, N.C. Tronson, Modulation of learning and memory by cytokines: Signaling mechanisms and long term consequences, Neurobiol. Learn. Mem. 115 (2014) 68–77 (Available at), ⟨https://www.sciencedirect.com/science/article/pii/S1074742714001543⟩.
[23] L. Doos, E.O. Roberts, N. Corp, U.T. Kadam, Multi-drug therapy in chronic condition multimorbidity: a systematic review, Fam. Pr. 31 (2014) 654–663 (Available at), ⟨https://www.ncbi.nlm.nih.gov/pmc/articles/PMC5942538/⟩.
[24] S. Elmore, Apoptosis: a review of programmed cell death, Toxicol. Pathol. 35 (2007) 495–516. ⟨https://www.ncbi.nlm.nih.gov/pmc/articles/PMC2117903/⟩.
[25] P.A. Engler, S.E. Ramsey, R.J. Smith, Alcohol use of diabetes patients: The need for assessment and intervention, Acta Diabetol. 50 (2013) 93–99 (Available at), ⟨https://www.ncbi.nlm.nih.gov/pmc/articles/PMC2954251/⟩.
[26] S. Ferlita, A. Yegiazaryan, N. Noori, G. Lal, T. Nguyen, K. To, V. Venketaraman, Type 2 diabetes mellitus and altered immune system leading to susceptibility to pathogens, especially mycobacterium tuberculosis, J. Clin. Med. 8 (2019) 2219. ⟨https://www.ncbi.nlm.nih.gov/pmc/articles/PMC6947370/⟩.
[27] S.L. Fink, B.T. Cookson, Apoptosis, pyroptosis, and necrosis: mechanistic description of dead and dying eukaryotic cells, Infect. Immun. 73 (2005) 1907–1916. ⟨https://www.ncbi.nlm.nih.gov/pmc/articles/PMC1087413/⟩.
[28] C. Gabay, Interleukin-6 and chronic inflammation, Arthritis Res. Ther. 8 (2006) S3, https://doi.org/10.1186/ar1917. Accessed May 10, 2022.
[29] U. Galicia-Garcia, A. Benito-Vicente, S. Jebari, A. Larrea-Sebal, H. Siddiqi, K. B. Uribe, H. Ostolaza, C. Martín, Pathophysiology of type 2 diabetes mellitus, Int. J. Mol. Sci. 21 (2020) 6275 (Available at), ⟨https://www.ncbi.nlm.nih.gov/pmc/articles/PMC7503727/⟩.
[30] B. Guthrie, B. Makubate, V. Hernandez-Santiago, T. Dreischulte, The rising tide of polypharmacy and drug-drug interactions: population database analysis 1995–2010, BMC Med. 13 (2015) 74, https://doi.org/10.1186/s12916-015-0322-7. Accessed July 16, 2022.
[31] J. Haorah, S.H. Ramirez, N. Floreani, S. Gorantla, B. Morsey, Y. Persidsky, Mechanism of alcohol-induced oxidative stress and neuronal injury, Free Radic. Biol. Med 45 (2008) 1542–1550 (Available at), ⟨https://www.ncbi.nlm.nih.gov/pmc/articles/PMC2605399/⟩.
[32] G.J. Harry, A.D. Kraft, Neuroinflammation and microglia: considerations and approaches for neurotoxicity assessment, Expert Opin. Drug Metab. Toxicol. 4 (2008) 1265–1277 (Available at), ⟨https://www.ncbi.nlm.nih.gov/pmc/articles/PMC2658618/⟩.
[33] N. Ho, M.S. Sommers, I. Lucki, Effects of diabetes on hippocampal neurogenesis: links to cognition and depression, Neurosci. Biobehav. Rev. 37 (2013) 1346–1362. ⟨https://www.ncbi.nlm.nih.gov/pmc/articles/PMC3788092/⟩.
[34] C.-C. Huang, C.-C. Lee, K.-S. Hsu, The role of insulin receptor signaling in synaptic plasticity and cognitive function, Chang Gung Med. J. 33 (2010) 115–125.
[35] B. Hussain, C. Fang, J. Chang, Blood–brain barrier breakdown: an emerging biomarker of cognitive impairment in normal aging and dementia, Front. Neurosci. (2021) 15. ⟨https://www.frontiersin.org/articles/10.3389/fnins.2021.688090⟩.
[36] K. Iglay, H. Hannachi, P. Joseph Howie, J. Xu, X. Li, S.S. Engel, L.M. Moore, S. Rajpathak, Prevalence and co-prevalence of comorbidities among patients with type 2 diabetes mellitus, Curr. Med. Res. Opin. 32 (2016) 1243–1252.
[37] Ishunina T.A., Bogolepova I.N., Swaab D.F., 2019. Increased Neuronal Nuclear and Perikaryal Size in the Medial Mamillary Nucleus of Vascular Dementia and Alzheimer's Disease Patients: Relation to Nuclear Estrogen Receptor α. DEM 47: 274–280 Available at: https://www.karger.com/Article/FullText/500244 [Accessed July 3, 2021].

[38] H.B. Jang, M.J. Go, S.I. Park, H.-J. Lee, S.B. Cho, Chronic heavy alcohol consumption influences the association between genetic variants of GCK or INSR and the development of diabetes in men: a 12-year follow-up study, Sci. Rep. 9 (2019) 20029. ⟨https://www.nature.com/articles/s41598-019-56011-y⟩.

[39] U. Kadam, I. Roberts, S. White, R. Bednall, K. Khunti, P. Nilsson, C. Lawson, Conceptualising multiple drug use in patients with comorbidity and multimorbidity: proposal for standard definitions beyond the term polypharmacy, J. Clin. Epidemiol. (2018) 106.

[40] S.-J. Kim, D.-J. Kim, Alcoholism and diabetes mellitus, Diabetes Metab. J. 36 (2012) 108–115.

[41] A. Kołota, D. Głąbska, M. Oczkowski, J. Gromadzka-Ostrowska, Influence of alcohol consumption on body mass gain and liver antioxidant defense in adolescent growing male rats, Int. J. Environ. Res. Public Health (2019) 16 (Available at), ⟨https://www.ncbi.nlm.nih.gov/pmc/articles/PMC6651161/⟩.

[42] S. Kumar, M. Jin, A. Ande, N. Sinha, P.S. Silverstein, A. Kumar, Alcohol consumption effect on antiretroviral therapy and HIV-1 pathogenesis: role of cytochrome P450 isozymes, Expert Opin. Drug Metab. Toxicol. 8 (2012) 1363–1375 (Available at), ⟨https://www.ncbi.nlm.nih.gov/pmc/articles/PMC4033313/⟩.

[43] J.X. Liu, S.B. Pinnock, J. Herbert, Novel control by the CA3 region of the hippocampus on neurogenesis in the dentate gyrus of the adult rat, PLoS One 6 (2011), e17562.

[44] Q. Ma, F. Vaida, J. Wong, C.A. Sanders, Y. Kao, D. Croteau, D.B. Clifford, A. C. Collier, B.B. Gelman, C.M. Marra, J.C. McArthur, S. Morgello, D.M. Simpson, R. K. Heaton, I. Grant, S.L. Letendre, CHARTER Group, Long-term efavirenz use is associated with worse neurocognitive functioning in HIV-infected patients, J. Neurovirol 22 (2016) 170–178.

[45] Masuku , 2019. HIV and antiretroviral therapy-induced metabolic syndrome in people living with HIV and its implications for care: A critical review. Available at: ⟨https://www.journalofdiabetology.org/article.asp?issn=2078–7685;year=2019;volume=10;issue=2;spage=41;epage=47;aulast=Masuku⟩ [Accessed May 17, 2021].

[46] S.A. Meda, K.A. Hawkins, A.D. Dager, H. Tennen, S. Khadka, C.S. Austad, R. M. Wood, S. Raskin, C.R. Fallahi, G.D. Pearlson, Longitudinal effects of alcohol consumption on the hippocampus and parahippocampus in college students, Biol. Psychiatry Cogn. Neurosci. Neuroimaging 3 (2018) 610–617 (Available at), ⟨https://www.ncbi.nlm.nih.gov/pmc/articles/PMC6062479/⟩.

[47] N.T. Milne, R.S. Bucks, W.A. Davis, T.M.E. Davis, R. Pierson, S.E. Starkstein, D. G. Bruce, Hippocampal atrophy, asymmetry, and cognition in type 2 diabetes mellitus, Brain Behav. 8 (2017), e00741 (Available at), ⟨https://www.ncbi.nlm.nih.gov/pmc/articles/PMC5853633/⟩.

[48] S.A. Morris, D.W. Eaves, A.R. Smith, K. Nixon, Alcohol inhibition of neurogenesis: a mechanism of hippocampal neurodegeneration in an adolescent alcohol abuse model, Hippocampus 20 (2010) 596–607.

[49] H. Nagano, S. Ito, T. Masuda, S. Ohtsuki, Effect of insulin receptor-knockdown on the expression levels of blood–brain barrier functional proteins in human brain microvascular endothelial cells, Pharm. Res. (2021), https://doi.org/10.1007/s11095-021-03131-8. Accessed June 28, 2022.

[50] S. Ohtsuki, H. Yamaguchi, Y. Katsukura, T. Asashima, T. Terasaki, mRNA expression levels of tight junction protein genes in mouse brain capillary endothelial cells highly purified by magnetic cell sorting, J. Neurochem 104 (2008) 147–154.

[51] F.N. Osuji, C.C. Onyenekwe, J.E. Ahaneku, N.R. Ukibe, The effects of highly active antiretroviral therapy on the serum levels of pro-inflammatory and anti-inflammatory cytokines in HIV infected subjects, J. Biomed. Sci. 25 (2018) 88, https://doi.org/10.1186/s12929-018-0490-9. Accessed August 20, 2021.

[52] G. Paxinos, C. Watson, The Rat Brain in Stereotaxic Coordinates: Hard Cover Edition, Elsevier, 2006.

[53] J. Pearson-Leary, E.C. McNay, Novel roles for the insulin-regulated glucose transporter-4 in hippocampally dependent memory, J. Neurosci. 36 (2016) 11851–11864.

[54] L. Qin, J. He, R.N. Hanes, O. Pluzarev, J.-S. Hong, F.T. Crews, Increased systemic and brain cytokine production and neuroinflammation by endotoxin following ethanol treatment, J. Neuroinflamm. 5 (2008) 10.

[55] J.L. Rains, S.K. Jain, Oxidative stress, insulin signaling and diabetes, Free Radic. Biol. Med. 50 (2011) 567–575. ⟨https://www.ncbi.nlm.nih.gov/pmc/articles/PMC3557825/⟩.

[56] L.P. Reagan, H.B. Cowan, J.L. Woodruff, G.G. Piroli, J.M. Erichsen, A.N. Evans, H. E. Burzynski, N.D. Maxwell, F.Z. Loyo-Rosado, V.A. Macht, C.A. Grillo, Hippocampal-specific insulin resistance elicits behavioral despair and hippocampal dendritic atrophy, Neurobiol. Stress 15 (2021), 100354. ⟨https://www.sciencedirect.com/science/article/pii/S235228952100062X⟩.

[57] K. Rehman, M.S.H. Akash, A. Liaqat, S. Kamal, M.I. Qadir, A. Rasul, Role of Interleukin-6 in development of insulin resistance and type 2 diabetes mellitus, Crit. Rev. Eukaryot. Gene Expr. 27 (2017) 229–236.

[58] C. Reinke, N. Buchmann, A. Fink, C. Tegeler, I. Demuth, G. Doblhammer, Diabetes duration and the risk of dementia: a cohort study based on German health claims data, Age Ageing 51 (2022) afab231, https://doi.org/10.1093/ageing/afab231. Accessed April 22, 2022.

[59] P. Rheeder, Type 2 diabetes: the emerging epidemic. South African, Fam. Pract. 48 (2006), 20–20.

[60] C. Richard, M. Wadowski, S. Goruk, L. Cameron, A.M. Sharma, C.J. Field, Individuals with obesity and type 2 diabetes have additional immune dysfunction compared with obese individuals who are metabolically healthy, BMJ Open Dia.b Res. Care 5 (2017), e000379 (Available at), ⟨https://drc.bmj.com/lookup/doi/10.1136/bmjdrc-2016-000379⟩.

[61] T.S. Salameh, W.G. Mortell, A.F. Logsdon, D.A. Butterfield, W.A. Banks, Disruption of the hippocampal and hypothalamic blood–brain barrier in a diet-induced obese model of type II diabetes: prevention and treatment by the mitochondrial carbonic anhydrase inhibitor, topiramate, Fluids Barriers CNS 16 (2019) 1, https://doi.org/10.1186/s12987-018-0121-6. Accessed May 9, 2022.

[62] J. Shi, J. Fan, Q. Su, Z. Yang, Cytokines and abnormal glucose and lipid metabolism, Front. Endocrinol. (2019) 10. ⟨https://www.frontiersin.org/articles/10.3389/fendo.2019.00703/full⟩.

[63] A.S. Smith, S. Ankam, R.C.B. Basa, K.L. Gordon, A.V. Terskikh, K.L. Jordan-Sciutto, J. Price, P.M. McDonough, HIV antiretrovirals have differential effects on viability and function in human iPSC-derived neurons and neural precursor cells, bioRxiv (2020), 2020.09.05.284422 Available at, ⟨https://www.biorxiv.org/content/10.1101/2020.09.05.284422v1⟩.

[64] M. Spinelli, S. Fusco, C. Grassi, Brain insulin resistance and hippocampal plasticity: mechanisms and biomarkers of cognitive decline, Front. Neurosci. 13 (2019). ⟨https://www.frontiersin.org/article/10.3389/fnins.2019.00788⟩.

[65] K.S. Tan, K.O. Lee, K.C. Low, A.M. Gamage, Y. Liu, G.-Y.G. Tan, H.Q.V. Koh, S. Alonso, Y.-H. Gan, Glutathione deficiency in type 2 diabetes impairs cytokine responses and control of intracellular bacteria, J. Clin. Investig. 122 (2012) 2289–2300. ⟨https://www.ncbi.nlm.nih.gov/pmc/articles/PMC3366396/⟩.

[66] P. Tien, M. Schneider, S. Cole, A. Levine, M. Cohen, J. Dehovitz, M. Young, J. Justman, Antiretroviral therapy exposure and insulin resistance in the Women's Interagency HIV study, J. Acquir. Immune Defic. Syndr. (1999) 49 (2008) 369–376.

[67] L.B. Tovar-y-Romo, N.N. Bumpus, D. Pomerantz, L.B. Avery, N. Sacktor, J. C. McArthur, N.J. Haughey, Dendritic spine injury induced by the 8-hydroxy metabolite of efavirenz, J. Pharmacol. Exp. Ther. 343 (2012) 696–703.

[68] A. Tseng, J. Seet, E.J. Phillips, The evolution of three decades of antiretroviral therapy: challenges, triumphs and the promise of the future, Br. J. Clin. Pharm. 79 (2015) 182–194 (Available at), ⟨https://www.ncbi.nlm.nih.gov/pmc/articles/PMC4309625/⟩.

[69] Y.-F. Tu, S.-T. Jiang, C.-W. Chiang, L.-C. Chen, C.-C. Huang, Endothelial-specific insulin receptor substrate-1 overexpression worsens neonatal hypoxic-ischemic brain injury via mTOR-mediated tight junction disassembly, Cell Death Discov. 7 (2021) 1–11. ⟨https://www.nature.com/articles/s41420-021-00548-3⟩.

[70] L.P. van der Heide, A. Kamal, A. Artola, W.H. Gispen, G.M.J. Ramakers, Insulin modulates hippocampal activity-dependent synaptic plasticity in a N-methyl-d-aspartate receptor and phosphatidyl-inositol-3-kinase-dependent manner, J. Neurochem. 94 (2005) 1158–1166.

[71] S.H. Vermund, E.K. Sheldon, M. Sidat, Southern Africa: the highest priority region for HIV prevention and care interventions, Curr. HIV/AIDS Rep. 12 (2015) 191–195.

[72] C.M.O. Volpe, P.H. Villar-Delfino, P.M.F. dos Anjos, J.A. Nogueira-Machado, Cellular death, reactive oxygen species (ROS) and diabetic complications, Cell Death Dis. 9 (2018) 1–9. ⟨https://www.nature.com/articles/s41419-017-0135-z⟩.

[73] D.R. Whiting, L. Guariguata, C. Weil, J. Shaw, IDF diabetes atlas: global estimates of the prevalence of diabetes for 2011 and 2030, Diabetes Res. Clin. Pract. 94 (3) (2011) 311–321. ⟨https://www.sciencedirect.com/science/article/pii/S0168822711005912⟩.

[74] R.D. Wilson, M.S. Islam, Fructose-fed streptozotocin-injected rat: an alternative model for type 2 diabetes, Pharmacol. Rep. 64 (2012) 129–139.

[75] W. Zhao, H. Chen, H. Xu, E. Moore, N. Meiri, M.J. Quon, D.L. Alkon, Brain insulin receptors and spatial memory. Correlated changes in gene expression, tyrosine phosphorylation, and signaling molecules in the hippocampus of water maze trained rats, J. Biol. Chem. 274 (1999) 34893–34902.

[76] U. Ziegler, P. Groscurth, Morphological features of cell death, N. Physiol. Sci. 19 (2004) 124–128.